



بسم الله الرحمن الرحيم

Sudan University of Science and Technology

Collage OF Graduate Studies

M.sc in biomedical engineering



A research title:

A Hybrid Technique for Speckle Noise Reduction In ultrasound images

عنوان البحث:

طريقة هجين للحد من ضوضاء الرقطة في صور الموجات فوق الصوتية

Prepared By:

NusibaAbdalelahHasabelrsool Ahmed

Supervised by:

Dr.Banazier Ahmed Ibrahim

August 2016

قال تعالى :

" و قل رب زدني علما "

صدق الله العظيم

سورة طه- آيه (114)

Dedication

Every challenging work needs self-efforts as well as guidance of elders specially those who were much closed to our heart.

My humble effort I dedicate to my sweet and loving

Mother and father

Whose affection, love encouragement and prays of day and night make able exceed this stage.

Along with all hard working and respected Teachers

Acknowledgement

The completion of this undertaking could not have been possible without assistance and guidance of so many people whose names may not all be enumerated. Their support is sincerely appreciated and gratefully acknowledged.

However, I would like to express deep appreciation and indebtedness particularly to supervisor

Dr. Banazier Ahmed Ibrahim for her endless support

To all relatives, friends and others who in one way or another shared their support, either morally, financially and physically. Thank you

Above all, to the great almighty, the author of knowledge and wisdom
Allah.

Table of Contents

No.	Content	Page No.
	Dedication	I
	Acknowledgement	II
	Table of contents	III
	List of tables	V
	List of figures	VII
	Abbreviations	IX
	Abstract	XI
	المستخلص	XII
Chapter One: introduction		
1.1	General view	1
1.2	Problem statement	1
1.3	Research objectives	2
1.4	Methodology	2
1.5	Thesis layout	2
Chapter Two: Theoretical Background		
2.1	Introduction	3
2.2	Basics of ultrasound	3
2.3	Types of ultrasound waves	4
2.4	The generation of ultrasound	5
2.4.1	Mainstream technologies	5
2.4.2	Transducers	5
2.4.3	Piezoelectricity	6
2.5	Beam forming	7
2.6	Ultrasound's interaction with the medium	8
2.6.1	Reflection	9
2.6.2	Scattering	10
2.6.3	Absorption	10
2.6.4	Attenuation	11
2.7	Imaging	12
2.8	Importance of ultrasound Imaging	15
2.9	Ultrasound Imaging System	16

No.	Content	Page No.
2.10	Speckles in Ultrasound Imaging	17
2.10.1	Speckle Noise	18
2.10.2	Speckle models	19
2.10.3	Need for Image Enhancement in Ultrasound Imaging	19
2.10.4	Speckle reduction methods	20
2.10.4.1	Compounding Methods	20
2.10.4.2	Post-Acquisition Methods	20
2.10.4.2.1	Single scale spatial filtering Methods	21
2.10.4.2.2	Multi scale Methods	21
2.10.4.2.2.1	Wavelet based speckle reduction methods	21
2.10.4.2.2.2	Pyramid based speckle reduction methods	22
2.10.5	An overview of the common Despeckle Filtering techniques	23
2.11	Wavelet Domain Noise Filtering	27
2.11.1	Brief history	27
2.11.2	Wavelet transforms	28
2.11.3	Discrete Wavelet Transform	28
2.11.4	Wavelet Decomposition	29
2.12	Image quality assessment	32
Chapter three		
	Literature review	34
Chapter four: Materials and Methodology		
4.1	The proposed method	39
4.2	The proposed method algorithm	40
4.3	The proposed method flow chart	41

No.	Content	Page No.
Chapter five: Results and Discussion		
5.1	Experimental Results	42
5.2	Discussion	75
Chapter six : Summary and Future work		
6.1	Conclusion	76
6.2	recommendations	77
	References	78

List of Tables

No. of table	Title	No. of page
Table 5.1	The measures of image quality evaluation metrics is computed for the liver image (with variance $\sigma_n = 0.05$) at statistical measurement of RMSE, SNR and PSNR for different filter types and for the proposed method.	48
Table 5.2	The measures of image quality evaluation metrics is computed for the liver image (with variance $\sigma_n = 0.5$) at statistical measurement of RMSE, SNR and PSNR for different filter types and for the proposed method.	53
Table 5.3	The measures of image quality evaluation metrics is computed for the fetal image (with variance $\sigma_n = 0.05$) at statistical measurement of RMSE, SNR and PSNR for different filter types and for the proposed method.	58
Table 5.4	The measures of image quality evaluation metrics is computed for the fetal image (with variance $\sigma_n = 0.5$) at statistical measurement of RMSE, SNR and PSNR for different filter types and for the proposed method.	63
Table 5.5	The measures of image quality evaluation metrics is computed for the abnormal GYN image (with variance $\sigma_n = 0.05$) at statistical measurement of RMSE, SNR and PSNR for different filter types and for the proposed method.	68

No. of table	Title	No. of page
Table 5.6	The measures of image quality evaluation metrics is computed for the abnormal GYN image (with variance $\sigma_n = 0.5$) at statistical measurement of RMSE, SNR and PSNR for different filter types and for the proposed method.	73

List of Figures

No. of figure	Title	No. of page
Figure2.1	sketch of the ultrasound interaction with tissue	12
Figure 2.2	Illustrate the image forming in ultrasound	13
Figure 2.3	Block diagram of Ultrasound Imaging System	16
Figure 2.4	show the wavelet analysis	29
Figure 2.5	show the 2D wavelet decomposition	29
Figure 2.6	show the subbands after one level of the image decomposition	30
Figure 2.7	Shows multi- stages reconstruction	32
Figure 4.1	show the flow chart of the proposed method	41
Figure 5.1	wavelet decomposition of the liver image with noise $\sigma_n = 0.05$ and $\sigma_n = 0.5$, respectively	43
Figure 5.2	wavelet decomposition of the fetal image with noise $\sigma_n = 0.05$ and $\sigma_n = 0.5$, respectively	43
Figure 5.3	wavelet decomposition of the abnormal GYN image with noise $\sigma_n = 0.05$ and $\sigma_n = 0.5$, respectively	44
Figure 5.4	results of liver image despeckled by various filters (variance $\sigma_n = 0.05$)	47
Figure 5.5	performance analysis graph for the computational results (IMQ) for the liver image ($\sigma_n = 0.05$)	49
Figure 5.6	results of liver image despeckled by various filters (variance $\sigma_n = 0.5$)	52
Figure 5.7	performance analysis graph for the computational results (IMQ) for the liver image ($\sigma_n = 0.5$)	54
Figure 5.8	results of fetal image despeckled by various filters (variance $\sigma_n = 0.05$)	57
Figure 5.9	performance analysis graph for the computational results (IMQ) for the fetal image ($\sigma_n = 0.05$)	59

No. of figure	Title	No. of page
Figure 5.10	results of fetal image despeckled by various filters (variance $\sigma_n=0.5$)	62
Figure 5.11	performance analysis graph for the computational results (IMQ) for the fetal image ($\sigma_n=0.5$)	64
Figure 5.12	results of abnormal GYN image despeckled by various filters (variance $\sigma_n=0.05$)	67
Figure 5.13	performance analysis graph for the computational results (IMQ) for the abnormal GYN image ($\sigma_n=0.05$)	69
Figure 5.14	results of abnormal GYN image despeckled by various filters (variance $\sigma_n=0.5$)	72
Figure 5.15	performance analysis graph for the computational results (IMQ) for the abnormal GYN image ($\sigma_n=0.5$)	74

Abbreviations

US	Ultrasound
IMQ	Image quality metrics
LL	Low –Low band
LH	Low –High band
HL	High – Low band
HH	High –High band
CT	Computed Tomography
MRI	Magnetic Resonance Imaging
US A-mode	Ultrasound Amplitude mode
US M-mode	Ultrasound Motion mode
US B-mode	Ultrasound Brightness mode
US TM-mode	Ultrasound Time-motion mode
US D-mode	Ultrasound Doppler mode
PZT	lead zirconatetitanate piezoelectric lead
PVDF	Polyvinylidenedifluoride piezoelectric lead
cMUTs	capacitive micromachined ultrasonic transducers
SAR	aperture radar imagery
SND	scatterer number density
FFS	Fully formed speckle
NRLR	Non randomly distributed with long-range order
NRSR	Non randomly distributed with short-range order
PDF	probability density function
PDE	partial differential equation
ad	anisotropic diffusion
MSE	Mean Square Error
RMSE	Root Mean Square Error
SNR	Signal to Noise Ratio
PSNR	Peak Signal to Noise Ratio
CC	Correlation Coefficient
SSI	Structure Similarity Index
QI	Image Quality Index
EPF	and Edge Preservation Factor
NCD	nonlinear coherent diffusion
DWT	discrete wavelet decomposition
CWT	continuous-time wavelet transform

IDWT	inverse discrete wavelet decomposition
SB-TS	sub-band tree structuring
WPD	wavelet packet decomposition
DsFlecasort	Neighborhood averaging
DsFlsmv	First Order Statistics Filtering
DsFlsminsc	Homogenous area filter
DsFca	linear scaling gray level filter
DsFls	the local statistics filter
DsFmedian	median filter
DsFsrاد	Speckle Reduction Anisotropic Diffusion filter
SRAD	Speckle Reduction Anisotropic Diffusion

Abstract

In the field of biomedical imaging, Ultrasound is an incontestable vital tool for diagnosis, it provides in non-invasive manner the internal structure of the body to detect eventually diseases or abnormalities tissues. These images are obtained with a simple linear or sector scan US probe, which show a granular appearance called speckle. . Unfortunately, the presence of speckle noise affects edges and fine details which limit the contrast resolution and make diagnostic more difficult. The removal of this noise is still a challenging one in medical image processing and analysis, because of multiplicative nature.

Most of speckle reduction techniques have been studied by researchers; however, there is no comprehensive method that takes all the constraints into consideration. Filtering is one of the common methods which are used to reduce the speckle noises. The objectives of this work was to carry out a comparative evaluation of despeckle filtering based on image quality evaluation metrics, moreover a hybrid technique has been proposed which works by passing an image through wavelet based Multiresolutional analysis and combined filtering techniques with SRAD filter (Speckle Reduction Anisotropic Diffusion) and hybrid median filters, for more improvement the total variation filter has been applied on the reconstructed image to get a final image. The quality of the enhanced images will be evaluated in terms of filter assessment parameters namely Signal-to-Noise Ratio (SNR), Peak Signal-to-Noise Ratio (PSNR), and Root Mean Square Error (RMSE) as well as in term of visual quality of the images for each tested filter. The computational results are presented in the form of filtered images, statistical tables and diagrams. Based on the statistical measures and visual quality of the filtered images the proposed method performed well over other conventional techniques.

المستخلص

في مجال التصوير الطبي الحيوي, تعتبر الموجات فوق الصوتية هي أداة حيوية لا تقبل الجدل للتشخيص فإنها توفر بطريقة لا تخترق البنية الداخلية للجسم الكشف عن الامراض والتشوهات في الانسجة الحيوية, ويتم الحصول علي هذه الصور بطريقة المسح الخطي أو المقطعي للموجات, والتي تؤدي لظهور حبيبات تسمى البقع أو الرقطة.

وجود ضوضاء الرقطة هذا يؤثر علي حواف الصورة والتفاصيل الدقيقة و بذلك تحد من تباين الصورة ووضوحها و بالتالي تجعل التشخيص أكثر صعوبة. إزالة هذه الضوضاء لايزال يعتبر تحديا في مجال معالجة و تحليل الصور الطبية و ذلك نسبة لطبيعته المعقدة.

أغلب التقنيات المستخدمة في تقليل هذه الضوضاء تمت دراستها من قبل الباحثين, ولكن لا توجد طريقة شاملة تأخذ كل القيود في عين الاعتبار, هذا البحث يقوم بتقديم دراسة مقارنة عامة لأداء عدد من المرشحات وفعاليتها في تقليل هذا النوع من الضوضاء و ذلك بناء علي المقاييس المستخدمة في تقييم جودة الصورة.

أيضا تهدف هذه الأطروحة لإقتراح تقنية للتقليل من أثر الضوضاء و تعزيز صور الموجات فوق الصوتية في المجال الطبي, هذه الطريقة مكونة من عدة مرشحات تعمل سويا في تسلسل للوصول للصورة المطلوبة.

تم استخدام مرشحين و هما مرشح الهجين المتوسط و مرشح الحد من ضوضاء الرقطة متباين الخواص و مرشح الانحراف الكلي في مجموعة مع تقنية تحليل الموجات.

و قد توصلنا في هذا البحث إلي أن الطريقة المقترحة هي الأفضل من حيث مقاييس تقييم جودة الصورة, لأنها تحافظ علي تفاصيل الصورة والحواف والملامح مقارنة بالطرق الأخرى لمشركات ضوضاء الرقطة.

Chapter One

Introduction

1.1 General view:

Ultrasound imaging system is an important imaging modality in medical diagnoses. Features like noninvasive nature, low cost, portability, and real-time image formation capacity are making this diagnostic tool attractive. Over the years, its application extended to include many fields and research is underway to improve the technology even further. One of the areas where research in this field has addressed is the fundamental problem of speckle noise, which is an interference effect caused by the scattering of the ultrasonic beam from microscopic tissues inhomogeneities. It considers as a major limitation that hampers the perception and the extraction of fine details from the image [1].

The removal of noise from image plays a vital role in medical image processing. Noise is generally grouped into two categories, image independent noise and image dependent noise. Still there is no general method for noise removal from an ultrasound image. It is to be noted that the noise removal is heavily based on edge information. Each and every approach has its own advantages and disadvantages. Therefore, the filters designed for image processing and analysis are required to yield sufficient noise reduction without losing the high frequency content of edges [2].

This work aims to suppress speckle in Ultrasound images, so a new approach for reduction is presented. These approaches combine two filters (total variation and hybrid median) with wavelet decomposition and reconstruct the image using inverse wavelet decomposition. The effectiveness of the method will be tested to achieve the enhancement.

1.2 Problem statement

One problem in processing ultrasound (US) images is the presence of speckle noise which is multiplicative due to containing diagnostic information that should be retained, and is a major limitation on image quality.

1.3 Research objectives

The general objective is:

The main objective of image denoising is necessary to remove such noises while retaining as much as possible the important signal feature.

The specific objective is:

1. To introduce a comparative study, that will compare the performance of the proposed filters against the other used filters.
2. To design an effective algorithm to reduce the noise-proposing a hybrid method, combining wavelet decomposition technique with SRAD filter, hybrid median filter and total variation filter.

1.4 Methodology

The research describes a hybrid technique for reducing such speckle noise. This algorithm is based on wavelet decomposition in combination with two filters. The proposed method works by analyzing the images using wavelet decomposition, which is produced 4-sub bands (LL, LH, HL, and HH).

The LL band passing through SRAD filter (Speckle Reduction Anisotropic Diffusion), while the other bands passes through a hybrid median filter and then the image is reconstructed using IDWT, for more finesse the resulted image passed through a total variation filter. The quality of the outputs measured by calculating the measures of the quality metrics which is compared with other IMQs values for other filtering technique to check the desire enhancement.

1.5 Thesis layout

This thesis falls into seven chapters. **Chapter One** introduces the research by highlighting the problem and objectives. **Chapter Two** adduces the ultrasound background, speckle noise and de-speckling importance. **Chapter Three** reviews the literature. **Chapter four** documents the research methodology. **Chapter**

five displays the results and discussion. Conclusion and recommendation are stated in **Chapter six**.

Chapter Two

Theoretical Background

2.1 Introduction

Ultrasound or ultrasonography is a medical imaging technique that uses high frequency sound waves and their echoes, Known as a “pulse echo technique”. The technique is similar to the echolocation used by bats, whales and dolphins, as well as SONAR used by submarines etc.

Medical imaging is an important source of diagnosing the malfunctions inside human body. Some crucial Medical imaging instruments are X-ray, Ultrasound, Computed Tomography (CT) ,and Magnetic Resonance Imaging (MRI). Medical ultrasound imaging is one of the significant techniques in detecting and visualizing the hidden body parts [3].

There could be distortions due to improper contact or air gap between the transducer probe and the human body. Another kind of distortion that may occur during ultrasound imaging is due to the beam forming process and also during the signal processing stage.

In order to overcome through various distortions, image processing has been successfully used. Image processing is a significant technique in medical field, especially in surgical decisions. Converting an image into homogeneous regions has been an area of hot research from a decade, especially when the image is made up of complex textures. Various techniques have been proposed for this task, including spatial frequency techniques. Image processing techniques have been used widely depending on the specific application and image modalities. Computer based detection of abnormal growth of tissues in a human body are preferred to manual processing methods in the medical investigations because of accuracy and satisfactory results. Several methods for processing the ultrasound images have been developed [3].

2.2 Basics of ultrasound

Ultrasound is sound with a frequency *above* the audible range which ranges from 20 Hz to 20 kHz. Sound is mechanical energy that needs a medium to propagate. Thus, in contrast to electromagnetic waves, it cannot travel in vacuum.

The frequencies normally applied in clinical imaging lies between 1 MHz and 20 MHz. The sound is generated by a transducer that first acts as a loudspeaker sending out an acoustic pulse along a narrow beam in a given direction. The transducer subsequently acts as a microphone in order to record the acoustic echoes generated by the tissue along the path of the emitted pulse. These echoes thus carry information about the acoustic properties of the tissue along the path. The emission of acoustic energy and the recording of the echoes normally take place at the same transducer, in contrast to CT imaging, where the emitter (the X-

ray tube) and recorder (the detectors) are located on the opposite side of the patient [4].

Ultrasound (as well as sound) needs a medium, in which it can propagate by means of local deformation of the medium. One can think of the medium as being made of small spheres (*e.g.* atoms or molecules), that are connected with springs. When mechanical energy is transmitted through such a medium, the spheres will oscillate around their resting position. Thus, the propagation of sound is due to a continuous interchange between kinetic energy and potential energy, related to the density and the elastic properties of the medium, respectively [4].

The two simplest waves that can exist in solids are *longitudinal* waves in which the particle movements occur in the same direction as the propagation (or energy flow), and *transversal* (or *shear* waves) in which the movements occur in a plane perpendicular to the propagation direction. In water and soft tissue the waves are mainly longitudinal. The frequency, f , of the particle oscillation is related to the wavelength, λ , and the propagation velocity c :

$$\lambda f = c \quad (2.1)$$

The sound speed in soft tissue at 37°C is around 1540 m/s, thus at a frequency of 7.5 MHz, the wavelength is 0.2 mm[4].

2.3 Types of ultrasound waves

Two simple waves, both are theoretical, since they need an infinitely large medium.

Since optical rays can be visualized directly, and since they behave in a manner somewhat similar to acoustic waves, they can help in understanding reflection, scattering and other phenomena taking place with acoustic waves. Therefore, there will often be made references to optics.

There are two types of waves that are relevant. They can both be visualized in 2D with a square acrylic water tank placed on an overhead projector:

- The plane wave which can be observed by shortly lifting one side of the container.

- The spherical wave, which can be visualized by letting a drop of water fall into the surface of the water.

When the plane wave is created at one side of the water tank, one will also be able to observe the reflection from the other side of the tank. The wave is reflected exactly as a light beam from a mirror or a billiard ball bouncing off the barrier of the table.

The spherical wave, that on the other hand, originates from a point source and propagates in all directions; it creates a complex pattern when reflected from the four sides of the tank[4].

2.4The generation of ultrasound

2.4.1 Mainstream technologies

In this section, the state of the art in the mainstream technologies which underpin the contemporary clinical applications of ultrasonic imaging is reviewed. The range of these technologies is now so great that it has been necessary to be selective in choosing those technologies which seem to be most important; it is hoped that this selection will not be thought to be too biased [5].

2.4.2Transducers

In some respects, the transducer is the most critical component in any ultrasonic imaging system. In other words, such is the state of the art in systems such as electronic circuitry and display technology that it is the performance of the transducer which determines how closely the limits imposed by the characteristics of the tissues themselves can be approached.

Nowadays, the transducers which are in clinical use almost exclusively use a piezoelectric material, of which the artificial ferroelectric ceramic, lead zirconatetitanate (PZT) is the most common. The ideal transducer for ultrasonic imaging would have a characteristic acoustic impedance perfectly matched to that of the (human) body; have high efficiency as a transmitter and high sensitivity as a receiver, a wide dynamic range and a wide frequency response for pulse operation. PZT has a much higher characteristic impedance than that of water but it can be made to perform quite well by the judicious use of matching layers consisting of materials with intermediate characteristic impedances. Even better performance can be obtained by embedding small particles or shaped structures of PZT in a plastic to form a composite material: this has lower characteristic impedance than that of PZT alone, although it has similar ferroelectric properties [5].

Polyvinylidenedifluoride (PVDF) is a plastic which can be polarized so that it has piezoelectric properties. The piezoelectric effect can be enhanced by the addition of small quantities of appropriate chemicals. The advantages of this material are that it has a relatively low characteristic impedance and broad frequency bandwidth; it is fairly sensitive as a receiver but rather inefficient as a transmitter.

Piezoelectric transducers are normally operated over a band of frequencies centered at their resonant frequency. The resonant frequency of a transducer occurs when it is half a wavelength in thickness. Typically, a PZT transducer resonant at a frequency of, say, 3 MHz is about 650 μm thick and this means that it is sufficiently mechanically robust for simple, even manual, fabrication techniques to be employed in probe construction. Higher frequency transducers are proportionally thinner and, consequently, more fragile.

The potential of capacitive micromachined ultrasonic transducers (cMUTs) at least partially to replace PZT and PVDF devices in ultrasonic imaging is the subject of current research. A cMUT consists of a micromachined capacitor, typically mounted on a silicon substrate and with a thin electroded membrane as the other plate of the capacitor: this acts as the active surface of the transducer. A dc voltage is applied between the plates of the device; the application of an AC voltage causes the membrane to transmit a corresponding oscillatory force, while a received wave causes a corresponding change in the spacing between the plates, thus generating an electrical signal. CMUTs are adequately sensitive as receivers, but need high voltages to be effective transmitters. Some of the potential advantages of these devices are that they can be fabricated into arrays with integrated electronics and, if manufactured in large quantities, could be relatively inexpensive.

Although some simple probes contain single-element transducers (e.g., one element for transmitting and one for receiving, in a continuous-wave Doppler system), most modern imaging systems use arrays of transducer elements for beam forming [5].

2.4.3 Piezoelectricity

The acoustic field is generated by using the piezo electric effect present in certain ceramic materials. Electrodes (e.g. thin layers of silver) are placed on both sides of a disk of such a material. One side of the disk is fixed to a damping so-called backing material, the other side can move freely. If a voltage is applied to the two electrodes, the result will be a physical deformation of the crystal surface, which will make the surroundings in front of the crystal vibrate and thus generate a sound field. If the material is compressed or expanded, as will be the case when an

acoustic wave impinges on the surface, the displacement of charge inside the material will cause a voltage change on the electrodes; this is used for emission and reception of acoustic energy, respectively [5].

2.5 Beam forming

In ultrasonic imaging, the beam may be scanned through the tissue either by mechanical movement of a single element or an annular array transducer, or by electronic control of a transducer array consisting of a number of small elements. For two-dimensional scanning, the array typically consists of 256 elements. The simplest arrangement is a linear array, within which an aperture is formed from, say, 16 contiguous elements and which is stepped along the array element by element to acquire an image with, in this example, 241 lines.

The same number of lines in a sector format can be acquired by curving the array into a segment of a cylinder. A sector scan can also be acquired by controlling the phases of the signals associated with each of the elements in the aperture. Whatever the arrangement, the application of distinct time delays to excite each element focuses the transmitted beam at a particular range. By transmitting several beams in the same position but with different foci, a sharply focused transmitted beam can be synthesized. On reception, the focus can be swept along the beam by dynamically changing the time delays associated with the active transducer elements, so that its position coincides continuously with that of the instantaneous origin of the echoes. Both when transmitting and receiving, the amplitudes of the signals associated with the active elements can be weighted to minimize the amplitudes of the beam side lobes, which are critical in determining the image contrast resolution. Also, the number of elements in the active aperture can be dynamically increased with increasing depth of penetration to maintain a constant f -number, within the limit imposed by the total length of the array and optimized to minimize the effect of tissue inhomogeneity.

For three-dimensional imaging, the two-dimensional scan plane produced by a one-dimensional linear, curved or phased array can be swept mechanically, either linearly in the orthogonal direction or through a sector. Recently, two-dimensional transducer arrays have been developed. Because of the very large number of transducer elements in these arrays, beam forming in three dimensions can be achieved more economically but with some degradation in performance by sparsely populating the array. For real-time three-dimensional scanning, several transmitting beams can be synthesized simultaneously; a single receiving beam can be associated with each transmitting beam, or, by increasing the width of each transmitting beam, several sharply focused receiving beams can be accommodated simultaneously in each transmitted beam.

The beam-forming time delays and aperture apodization functions are digitally controlled.

The sampling frequency has to be at least twice the highest ultrasonic frequency, in order to avoid aliasing. Further improvement can be obtained by applying a finite impulse response digital filter or by demodulating the radio-frequency signals to baseband to obtain quadrature signals so that the associated time delays can be finely adjusted by phase rotation.

An intriguing development in high-speed imaging has recently been brought about by the application of limited diffraction beams. A limited diffraction beam can be produced by appropriate excitation of a transducer array. Following the transmission of a single plane wave pulse, the received signals are weighted with limited diffraction beams simultaneously to produce multiple A-lines which can be used to create a complete two-dimensional image [5].

2.6 Ultrasound's interaction with the medium

The interaction between the medium and the ultrasound emitted into the medium can be described by the following phenomena:

The echoes that travel back to the transducer and thus give information about the medium is due to two phenomena: *reflection* and *scattering*. Reflection can be thought of as when a billiard ball bounces off the barrier of the table, where the angle of reflection is identical to the angle of incidence. Scattering (Danish: *spredning*) can be thought of, when one shines strong light on the tip of a needle: light is scattered in all directions. In acoustics, reflection and scattering is taking place when the emitted pulse is travelling through the interface between two media of different acoustic properties, as when hitting the interface of an object with different acoustic properties.

Specifically, reflection is taking place when the interface is large relative to the wavelength (*e.g.* between blood and intima in a large vessel). Scattering is taking place when the interface is small relative to the wavelength (*e.g.* red blood cell).

The abstraction of a billiard ball is not complete, however: In medical ultrasound, when reflection is taking place, typically only a (small) part of the wave is reflected. The remaining part is *transmitted* through the interface. This transmitted wave will nearly always be *refracted*, thus typically propagating in another direction. The only exception is when the wave impinges perpendicular on a large planar interface: The reflected part of the wave is reflected back in exactly the same direction as it came from (like with a billiard ball) and the refracted wave propagates in the same way as the incident wave.

Reflection and scattering can happen at the same time, for instance, if the larger planar interface is rough. The smoother, the more it resembles pure reflection (if it is completely smooth, *specular reflection* takes place). The rougher, the more it resembles scattering.

When the emitted pulse travels through the medium, some of the acoustic (mechanical) energy is converted to heat by a process called *Absorption*. Of course, also the echoes undergo absorption.

Finally, the loss in intensity of the forward propagating acoustic pulse due to reflection, refraction, scattering and absorption is under one named *attenuation*[5].

2.6.1 Reflection

The reflection of ultrasound pulses by structures within the body is the interaction that creates the ultrasound image. The reflection of an ultrasound pulse occurs at the interface, or boundary, between two dissimilar materials, as shown in the following figure. In order to form a reflection interface, the two materials must differ in terms of a physical characteristic known as acoustic impedance Z . Although the traditional symbol for impedance, Z , is the same symbol used for atomic number, the two quantities are in no way related. Acoustic impedance is a characteristic of a material related to its density and elastic properties. Since the velocity is related to the same material characteristics, a relationship exists between tissue impedance and ultrasound velocity. The relationship is such that the impedance, Z , is the product of the velocity, v , and the material density, Y , which can be written as:

$$\text{Impedance} = (Y) (v) \quad (2.2)$$

The Production of an Echo and Penetrating Pulse at a Tissue Interface At most interfaces within the body, only a portion of the ultrasound pulse is reflected. The pulse is divided into two pulses, and one pulse, the echo, is reflected back toward the transducer and the other penetrates into the other material, as shown in the above figure. The brightness of a structure in an ultrasound image depends on the strength of the reflection, or echo. This in turn depends on how much the two materials differ in terms of acoustic impedance. The amplitude ratio of the reflected to the incident pulse is related to the tissue impedance values by

$$\text{Reflection loss (dB)} = 20 \log (Z_2 - Z_1)/(Z_2 + Z_1) \quad (2.3)$$

At most soft tissue interfaces, only a small fraction of the pulse is reflected. Therefore, the reflection process produces relatively weak echoes. At interfaces between soft tissue and materials such as bone, stones, and gas, strong reflections are produced [4].

2.6.2 Scattering

While reflection takes place at interfaces of infinite size, scattering takes place at small objects with dimensions much smaller than the wavelength. Just as before, the specific acoustic impedance of the small object must be different from the surrounding medium. The scattered wave will be more or less spherical, and thus propagate in all directions, including the direction towards the transducer. The latter is denoted backscattering.

The scattering from particles much less than a wavelength is normally referred to as Rayleigh scattering. The intensity of the scattered wave increases with frequency to the power of four.

Biologically, scattering can be observed in most tissue and especially blood, where the red blood cells are the predominant cells. They have a diameter of about 7 μm , much smaller than the wavelength of clinical ultrasound [5].

2.6.3 Absorption

Absorption is the conversion of acoustic energy into heat. The mechanisms of absorption are not fully understood, but relate, among other things, to the frictionloss in the springs, pure absorption can be observed by sending ultrasound through a viscous liquid such as oil [5].

2.6.4 Attenuation

The Reduction of Pulse Amplitude by Absorption of Its Energy As the ultrasound pulse moves through matter, it continuously loses energy. This is generally referred to as attenuation. Several factors contribute to this reduction in energy. One of the

most significant is the absorption of the ultrasound energy by the material and its conversion into heat. Ultrasound pulses lose energy continuously as they move through matter. This is unlike x-ray photons, which lose energy in "one-shot" photoelectric or Compton interactions. Scattering and refraction interactions also remove some of the energy from the pulse and contribute to its overall attenuation, but absorption is the most significant.

The rate at which an ultrasound pulse is absorbed generally depends on two factors: (1) the material through which it is passing, and (2) the frequency of the ultrasound. The attenuation (absorption) rate is specified in terms of an attenuation coefficient in the units of decibels per centimeter. Since the attenuation in tissue increases with frequency, it is necessary to specify the frequency when an attenuation rate is given. The attenuation through a thickness of material, x is given by:

$$\text{Attenuation (dB)} = (a) (f) (x) \quad (2.4)$$

Where (a) is the attenuation coefficient (in decibels per centimeter at 1 MHz), and (f) is the ultrasound frequency, in megahertz [6].

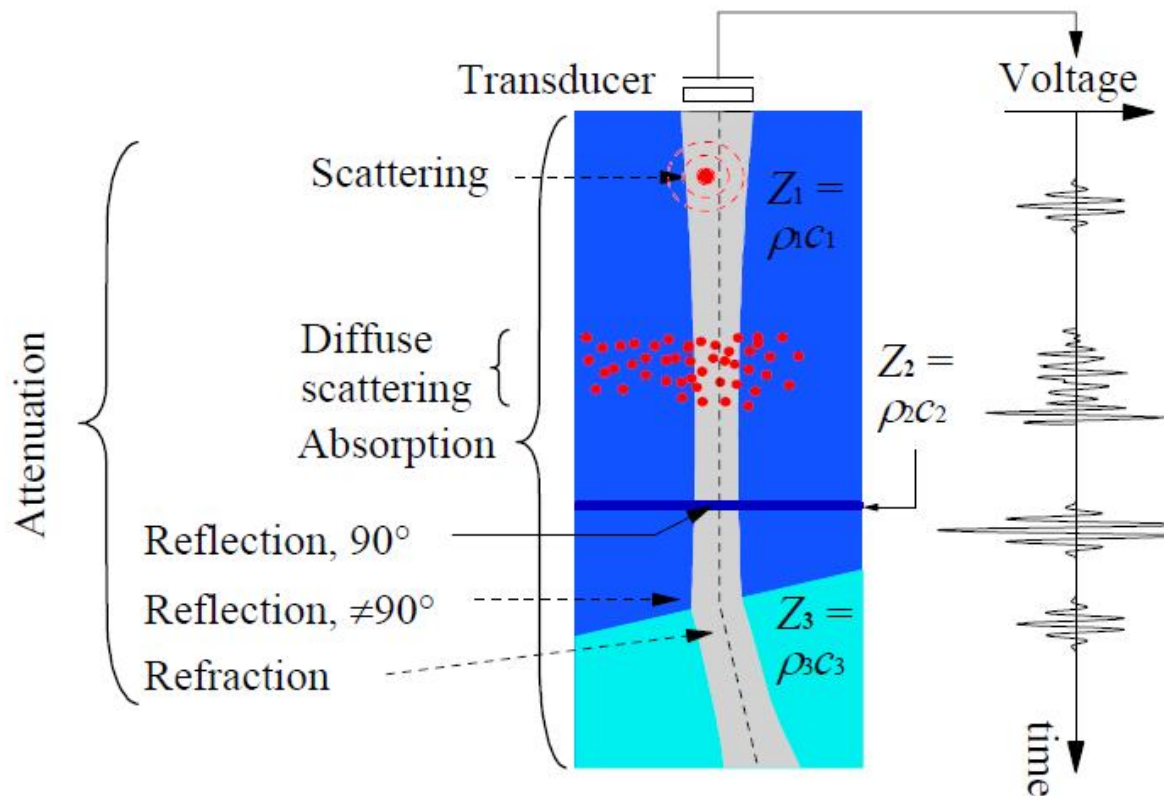


Figure 2.1: sketch of the ultrasound interaction with tissue [5].

2.7 Imaging

The basic principle behind pulse-echo imaging an acoustic pulse is emitted from the transducer, scattered by the point reflector and received after a time interval which is equal to the round trip travel time. The emitted pulse is also present in the received signal due to limitations of the electronics controlling the transducer. Right: the signal processing creating the envelope of the received signal followed by calculation of the logarithm yielding the scan line.

Imaging is based on the pulse-echo principle: A short ultrasound pulse is emitted from the transducer. The pulse travels along a beam pointing in a given direction. The echoes generated by the pulse are recorded by the transducer. This electrical signal is always referred to as the received signal. The later an echo is received, the

deeper is the location of the structure giving rise to the echo. The larger the amplitude of the echo received, the larger is the average specific acoustic impedance difference between the structure and the tissue just above. An image is then created by repeating this process with the beam scanning the tissue.

All this will now be considered in more detail by considering how Amplitude mode, Motion mode and Brightness mode work [5].

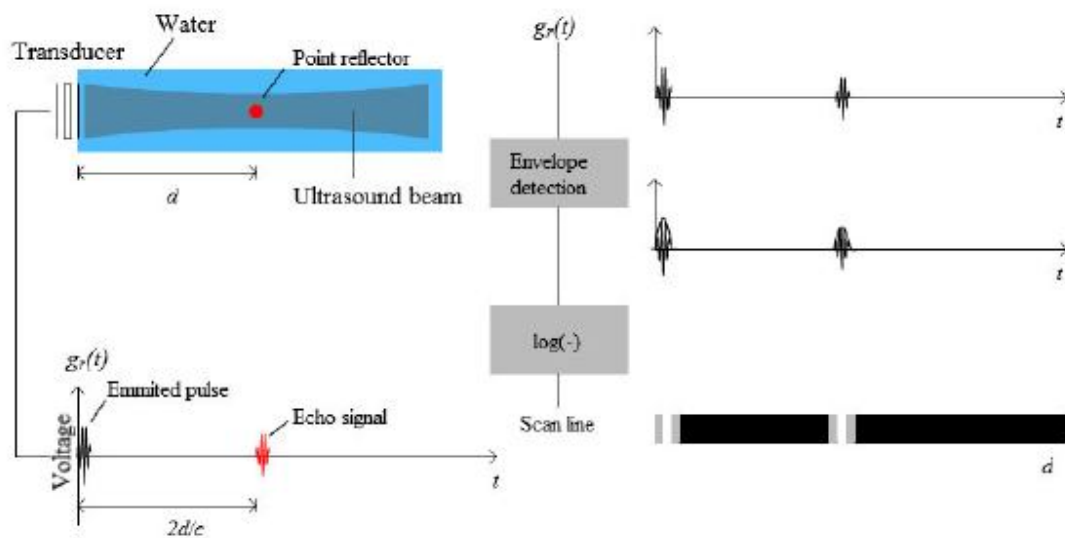


Figure 2.2: illustrate the image forming in ultrasound [5].

There are several options to form an image from this pulse-echo signal:

A-mode

A single point scatterer is located in front of the transducer at depth d . A short pulse is emitted from the transducer, and at time $2d/c$, the echo from the point target is received by the same transducer. Thus, the deeper the point scatterer is positioned, the later the echo from this point scatterer arrives. If many point scatterers (and reflectors) are located in front of the transducer, the total echo can be found by simple superposition of each individual echo, as this is a linear system, when the pressure amplitude is sufficiently low.

The *scan line* is created by calculating the envelope of the received signal followed by calculation of the logarithm, in order to compress the range of image values for

a better adoption to the human eye. So, the scan line can be called a *gray scale line*. The M-mode and B-mode images are made from scan lines [4].

M-mode

If the sequence of pulse emission and reception is repeated infinitely, and the scan lines are placed next to each other (with new ones to the right), *motion mode*, or M-mode, is obtained. The vertical axis will be depth in meters downwards, while the horizontal axis will be time in seconds pointing to the right. This mode can be useful when imaging heart valves, because the movement of the valves will make distinct patterns in the “image” [4].

B-mode

Brightness or B-mode is obtained by physically moving the scan line to a number of adjacent locations. The transducer is moved in steps mechanically across the medium to be imaged. Typically 100 to 300 steps are used, with spacing between 0.25λ and 5λ at each step; a short pulse is emitted followed by a period of passive registration of the echo. In order to prevent mixing the echoes from different scan lines, the registration period has to be long enough to allow all echoes from a given emitted pulse to be received [4].

TM-mode:

Time motion diagrams visualize movements of sound-reflecting tissue borders. This mode offers functional rather than morphological inspection [7].

D-mode:

The doppler mode makes use of the doppler effect (i.e., a shift in frequency that occurs if the source of sound, the receptor, or the reflector is moved) in measuring and visualizing blood flow. Several visualization modes are used:

1. Color Doppler: The velocity information is presented as a color-

- coded overlay on top of a B-mode image;
2. Continuous Doppler: Doppler information is sampled along a line through the body, and all velocities detected at each point in time are presented (on a time line).
 3. PW Doppler: Pulsed-wave Doppler information is sampled from only a small sample volume (defined in the 2D B-mode image), and presented on a time line.
 4. Duplex: Color and (usually) PW Doppler are simultaneously displayed [7].

2.8 Importance of ultrasound Imaging

ULTRASOUND imaging application in medicine and other fields is enormous. It has several advantages over other medical imaging modalities. The use of ultrasound in diagnosis is well established because of its noninvasive nature, low cost, capability of forming real time imaging and continuing improvement in image quality. It is estimated that one out of every four medical diagnostic image studies in the world involves ultrasonic techniques. US waves are characterized by frequency above 20 KHz which is the upper limit of human hearing. In medical US applications, frequencies are used between 500 KHz and 30 MHz. B-mode imaging is the most used modality in medical US. An US transducer which is placed onto the patient's skin over the imaged region sends an US pulse which travels along a beam into the tissue. Due to interfaces some of the US energy is reflected back to the transducer which converts it into echo signals. These signals are then sent into amplifiers and signal processing circuits in the imaging machine's hardware to form a 2-D image. This process of sending pulses launched in different directions is repeated in order to examine the whole region in the body. Thus, US imaging involves signals which are obtained by coherent summation of echo signals from scatterers in the tissue. In many cases volume quantification is important in assessing the progression of diseases and tracking progression of response to treatment. Thus, 3D ultrasound imaging has drawn great attention in recent years [8].

2.9 Ultrasound Imaging System

Figure (2.3) shows a functional block diagram of an ultrasound imaging system. The construction of ultrasound B-mode image involves capturing the echo signal returned from tissue at the surface of piezoelectric crystal transducers. These transducers convert the ultrasonic RF mechanical wave into electrical signal. Convex ultrasound probes collect the echo from tissue in a radial form. Each group of transducers is simultaneously activated to look at a certain spatial direction from which they generate a raw line signal (stick) to be used later for raster image construction. These sticks are then demodulated and logarithmically compressed to reduce their dynamic range to suit the commercial display devices. The final Cartesian image is constructed from the sampled sticks in a process called scan conversion.

Speckle reduction techniques can be applied on envelope detected data, log compressed data or on scan converted data. However, slightly different results will be produced for each data. In the compression stage some useful information about the imaged object may be deteriorated or even lost. However, any processing which works with envelope detected data has more information at its disposal and preserves more useful information. Compared to processing the scan converted image, envelope detected data has fewer pixels and thus incurs lower computational cost.

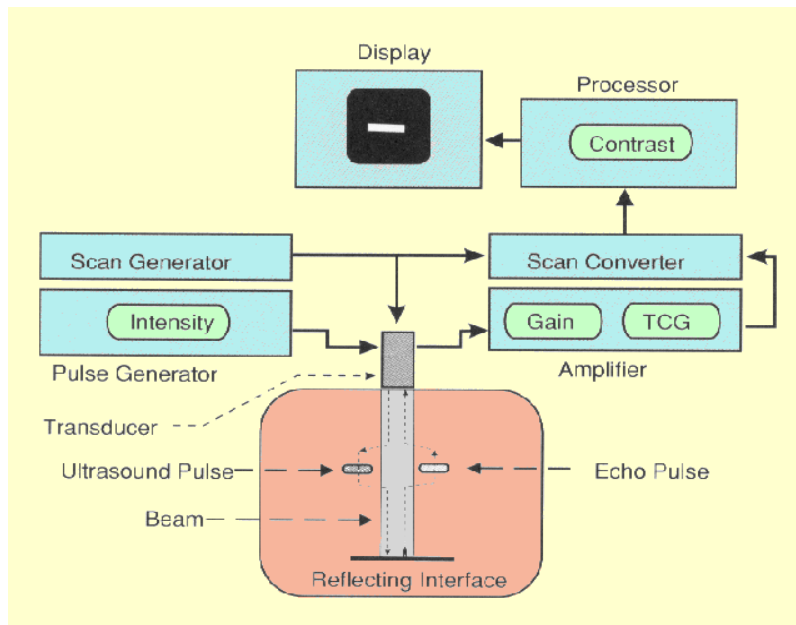


Figure 2.3: Block diagram of Ultrasound Imaging System [6].

For optimum result envelope detected data processing is preferred because some information that lost after the compression stage cannot be recovered by working with log compressed data or the scan converted image. However, the real time speckle reduction methods are applied on the scan converted image, since the scan converted image is always accessible where most commercial ultrasound systems do not output the envelope detected or log compressed data[8].

2.10 Speckles in Ultrasound Imaging

Noise is considered to be any measurement that is not part of the phenomena of interest. Images are prone to different types of noises. Departure of ideal signal is generally referred to as noise. Noise arises as a result of unmodelled or unmodellable processes going on in the production and capture of real signal. It is not part of the ideal signal and may be caused by a wide range of sources [9].

Moreover, there are different types of noise, for example the x- ray images are often corrupted by poisson noise, while the ultrasound images are affected by speckle noise. Speckle is a complex phenomenon, which degrades the image quality with a back scattered wave appearance which originates from many microscopic diffused reflections that passing through internal organs and make it more difficult for the observer to discriminate fine details of the image in diagnostic examinations. Thus, de-noising or reducing these speckle noise from a noisy image has become the predominant step in medical image processing [8].

Speckle in US B-scans is seen as a granular structure which is caused by the constructive and destructive coherent interferences of back scattered echoes from the scatterers that are typically much smaller than the spatial resolution of medical ultrasound system. This phenomenon is common to laser, sonar and synthetic aperture radar imagery (SAR). Speckle pattern is a form of multiplicative noise and it depends on the structure of imaged tissue and various imaging parameters.

Speckle degrades the target detectability in B-scan images and reduces the contrast, resolutions which affect the human ability to identify normal and pathological tissue. It also degrades the speed and accuracy of ultrasound image processing tasks such as segmentation and registration [8].

The nature of the speckle pattern can be categorized into one of three classes according to the number of scatterers per resolution cell or the so called

scatterer number density (SND), spatial distribution and the characteristics of the imaging system itself.

These classes are described as follows:

1. FFS (Fully formed speckle) pattern, which occurs when many fine randomly distributed scattering sites exist within the resolution cell of the pulse-echo system. In this case, the amplitude of the backscattered signal can be modeled as a Rayleigh distributed random variable with a constant SNR of 1.92. Under such conditions, the textural features of the speckle pattern represent a multivariate signature of the imaging instrument and its point spread function. Blood cells are typical examples of this type of scatterers.
2. Non randomly distributed with long-range order (NRLR). Examples of this type are the lobules in liver parenchyma. It contributes a coherent or specular backscattered intensity that is in itself spatially varying. Due to the correlation between scatterers, the effective number of scatterers is finite. This situation can be modeled by the K-distribution. This type is associated with SNR below 1.92. It can also be modeled by the Nakagami distribution.
3. Non randomly distributed with short-range order (NRSR). Examples of this type include organ surfaces and blood vessels. When a spatially invariant coherent structure is present within the random scatterer region, the probability density function (PDF) of the backscattered signals becomes close to the Rician distribution. This class is associated with SNR above 1.92 [10].

2.10.1 Speckle Noise

It is a common form of noise that known as data drop-out noise commonly referred to as Speckle noise. Speckle is not a noise in an image but noise-like variation in contrast. This noise is, in fact, caused by errors in data transmission. The Corrupted pixels are either set to the maximum value, which is something like a snow in image or have single bits flipped over [9]. It arises from random Variations in the strength of the backscattered waves from objects and is seen mostly in medical imaging.

Nature of Speckle pattern depends on the number of scatters per resolution cell or scatter number density. Spatial distribution and the characteristics of the imaging system can be divided into three classes:

- a) The fully formed speckle pattern occurs when many random distributed scattering exists within the resolution cell of the imaging system. Blood cells are the example of this class.

b) The second class of tissue scatters is no randomly distributed with long-range order; Example of this type is lobules in liver parenchyma [11].

2.10.2 Speckle models

Although the existing despeckling filters are termed as edge and feature preserving filters some major limitation exists

- i. The filters are sensitive to the noise components
 - ii. Noise attenuation is not sufficient especially in the smooth and background areas
 - iii. The existing filters do not enhance edges but they only inhibit smoothing near edges
- Thus, effective despeckling requires an accurate statistical model of ultrasound signals. A generalized model of the speckle imaging can be written as:

$$g = fn + m \quad (2.5)$$

Let g denote the observed signal, m, n respectively the multiplicative and additive components of noise introduced by the acquisition process and f the original signal without noise. Generally the effect of additive noise is very small compared to multiplicative noise, So the simplified noise model :

$$g = fn \quad (2.6)$$

The statistics of speckle noise can be categorized into different classes according to Number of scatterers per resolution cell called scatterer number density (SND). In the case of many fine randomly distributed scatterers per resolution cell (>10) the speckle can be modeled by a Rayleigh distribution with a SNR of 1.92. When the scatterer densities are smaller a generalized version of Rayleigh distribution called the K-distribution can be used. For high SNR the Rician model can be used for lower the speckle can be modeled using Homodyne K-distribution more analytical models including [8].

2.10.3 Need for Image Enhancement in Ultrasound Imaging

Image enhancement has played a vital role in improving the image quality and reducing artefacts such as noise reduction from average image, simple algorithms for enhancing edges and adjustment of gray levels to boost contrast resolution.

Thus, speckle is considered as the dominant source of noise in ultrasound imaging and should be processed without affecting important image features.

Image processing in ultrasound images is used for various reasons:

- i. Ultrasound images are more complex as there are large number of image characteristics which includes diagnostic and artifactual.
- ii. Medical professionals resist to a processed appearance and are scared of loss of data or variation in diagnostic criteria.
- iii. As there are large number of clinical applications therefore computational power essential for real time (20–60 frames/s) image rates [12].

2.10.4 Speckle reduction methods

Several techniques have been proposed for despeckling in medical ultrasound imaging. In this section we present the classification and theoretical overview of existing despeckling techniques [13].

2.10.4.1. Compounding Methods

In this method a series of ultrasound images of the same target are acquired from different scan directions and with different transducer frequencies or under different strains. Then the images are averaged to form a composite image.

The compounding method can improve the target detectability but they suffer from degraded spatial resolution and increased system complexity [8].

2.10.4.2. Post-Acquisition Methods

This method does not require many hardware modifications. The post-acquisition image processing technique falls under two categories

(1) Single scale spatial filtering

(2) Multi-scale Methods

2.10.4.2.1 Single scale spatial filtering Methods

A speckle reduction filter that changes the amount of smoothing according to the ratio of local variance to local mean was developed. In that method, smoothing is increased in homogeneous regions where speckle is fully developed and reduced or even avoided in other regions to preserve details.

An unsharp masking filter was suggested in which the smoothing level is adjusted depending on the statistics of log compressed images. The above mentioned filters have difficulty in removing speckle near or on image edges.

Recently proposed filter utilizing short line segments in different angular orientations and selecting the orientation that is most likely to represent a line in the image. This technique poses a tradeoff between effective line enhancement and speckle reduction.

Numbers of Region growing based spatial filtering methods have been proposed. In these methods, it is assumed that pixels that have similar gray level and connectivity are related and likely to belong to the same object or region. After all pixels are allocated to different groups, spatial filtering is performed based on the local statistics of adaptive regions whose sizes and shapes are determined by the information content of the image.

The main difficulty in applying region growing based methods is how to design appropriate similarity criteria for region growing [8].

2.10.4.2.2 Multi scale Methods

Several multi scale methods based on wavelet and pyramid have been proposed for speckle reduction in ultrasound imaging.

2.10.4.2.1 Wavelet based speckle reduction methods

The wavelet based speckle reduction method usually includes:

- (1) Logarithmic transformation

- (2) Wavelet transformation
- (3) Modification of noisy coefficients using shrinkage function
- (4) Invert wavelet transform and
- (5) Exponential transformation. This method can be classified into three groups:

1. **Thresholding methods** - The wavelet coefficients smaller than the predefined threshold are regarded as contributed by noise and then removed. The thresholding techniques have difficulty in determining an appropriate threshold.

- 1. **Bayesian estimation methods** – This Method approximates the noise free signal based on the distribution model of noise free signal and that of noise. Thus, reasonable distribution models are crucial to the successful application of these techniques to medical ultrasound imaging
- 2. **Coefficients correlation methods** - This is an undecimated or over complete wavelet domain denoising method which utilizes the correlation of useful wavelet coefficients across scales. However this method does not rely on the exact prior knowledge of the noise distribution and this method is more flexible and robust compared to other wavelet based methods [8].

2.10.4.2.2 Pyramid based speckle reduction methods

Pyramid transform has also been used for reducing speckle. Approximation and interpolation filters in pyramid transform have low pass properties so that pyramid transform does not require quadrature mirror filters unlike sub band decomposition in wavelet transform

A ratio laplacian pyramid was introduced by considering the multiplicative nature of speckle. This method extended the conventional Kaun filter to multi scale domain by processing the interscale layers of the ratio laplacian pyramid. But this method differs from the need to estimate the noise variance in each interscale layers.

A speckle reduction method based on nonlinear diffusion filtering of band pass ultrasound images in the laplacian pyramid domain has been proposed which effectively suppresses the speckle while preserving edges and detailed features [8].

2.10.5 An overview of the common Despeckle Filtering techniques

A. Local Statistics Filtering

Most of the techniques for speckle reduction filtering in the literature use local statistics. Their working principle may be described by a weighted average calculation using subregion statistics to estimate statistical measures over different pixel windows varying from 3×3 up to 15×15 .

1. First Order Statistics Filtering (lsmv, wiener):

The filters using the first order statistics such as the variance and the mean of the neighborhood. Hence, the algorithms in this class may be traced back to the following equation:

$$f_{i,j} = g + k_{i,j} (g_{i,j} - g) \quad (2.7)$$

Where $f_{i,j}$ is the estimated noise-free pixel value, $g_{i,j}$ is the noisy pixel value in the moving window, g is the local mean value of an $N_1 \times N_2$ region surrounding and including pixel $g_{i,j}$, $k_{i,j}$ is a weighting factor with $k \in [0..1]$, and i, j , are the pixel coordinates. The factor $k_{i,j}$ is a function of the local statistics in a moving window.

2. Homogeneous Mask Area Filtering:

Is a 2-D filter operating in a 5×5 pixel neighborhood by searching for the most homogenous neighborhood area around each pixel, using a 3×3 subset window. The middle pixel of the 5×5 neighborhood is substituted with the average gray level of the 3×3 mask with the smallest speckle index C [14].

The window with the smallest C is the most homogenous semiwindow, which presumably does not contain any edge. The filter is applied iteratively until the gray levels of almost all pixels in the image do not change.

B. Median Filters:

In image processing the best known order statistics filter is the median filter and it is the simplest technique which is used to remove speckle noise, pulse noise or spike noise from the image. While other smoothing filters only remove noise from the signal but they are not able to preserve edges of the signal but median filter is the special smoothing filter which improves the result of later processing by removing noise from the signal and additionally preserves the edges. It is a simple nonlinear operator that replaces the middle pixel in the window with the median-value of its neighbors. The moving window for the median filter was 7×7 . It follows an algorithm in which each entry of the signal is replaced one by one with median of neighboring entries and median is calculated by replacing the pixel value with the middle pixel value and such a pattern of neighboring entries forms a sliding window which slides over entire signal one by one [12].

They are utilized for despeckling due to their robustness against impulsive type noise and edge preserving characteristics. The median filter produces less blurred images. The compounding procedure uses both the mean and median filters [8].

C. Hybrid Median Filter

The hybrid median filter is another modification of median filter. This filter is also called as corner preserving median filter is a three-step ranking operation. In a 5×5 pixel neighborhood, pixels can be ranked in two different ways. The median values of the 45 neighbors forming an “X” and the 90 neighbors forming a “+” are compared with the central pixel and the median value of that set is then saved as the new pixel value. The three step ranking operation does not impose a serious computational penalty as in the case of median filter. Each of the ranking operations is for a much smaller number of values than used in a square region of the same size. Even with the additional logic and manipulation of values, the hybrid method is faster than the conventional median. This median filter overcomes the tendency of median and truncated median filters to erase lines which are narrower than the half width of the neighborhood and to round corners [15].

D. Geometric Filtering

The concept of the geometric filtering is that speckle appears in the image as narrow walls and valleys. The geometric filter, through iterative repetition, gradually tears down the narrow walls (bright edges) and fills up the narrow valleys (dark edges), thus smearing the weak edges that need to be preserved.

It compares the intensity of the central pixel in a 3×3 neighborhood with those of its eight neighbors and, based upon the neighborhood pixel intensities, it increments or decrements the intensity of the central pixel such that it becomes more representative of its surroundings [14].

E. Diffusion Filtering

Diffusion filters remove noise from an image by modifying the image via solving a partial differential equation (PDE). The smoothing is carried out, depending on the image edges and their directions. Anisotropic diffusion is an efficient, nonlinear technique for simultaneously performing contrast enhancement and noise reduction. It smooths homogeneous image regions but retains image edges without requiring any information from the image power spectrum.

Modifying the image according to this linear isotropic diffusion equation is equivalent to filtering the image with a Gaussian filter. In this section we will present conventional anisotropic diffusion (ad) and coherent nonlinear anisotropic diffusion [14].

1. Anisotropic Diffusion Filtering:

Perona and Malik replaced the classical isotropic diffusion equation, that smooths the original image while trying to preserve brightness discontinuities. It increases smoothing parallel to the edge and stops smoothing perpendicular to the edge, as the highest gradient values are perpendicular to the edge and dilated across edges [14].

2. SRAD FILTER:

SRAD filter is known as speckle reducing anisotropic diffusion. The SRAD can eliminate speckle without distorting useful image information and without destroying the important image edges.

The SRAD PDE exploits the instantaneous coefficient of variation in reducing the speckle. [16].

F. Wavelet Filtering

Speckle reduction filtering in the wavelet domain, used in this study, is based on the idea of the DaubenchiesSymletwavelet and on soft-thresholdingdenoising, first proposed by Donoho. The method was also investigated by the dubenchies family of wavelets, although not perfectly symmetrical, were designed to have the least asymmetry and highest number of vanishing moments for a given compact support [14]. The wavelet filter, implemented in this study is described as follows:

- Estimate the variance of the speckle noise, σ^2n , from the logarithmic transformed noisy image.
- Compute the discrete wavelet transform (DWT), using the dubenchies wavelet for 8scales (db8).
- For each subband– Compute a threshold– Apply the thresholding procedure on the wavelet coefficients.
- Invert the multiscale decomposition to reconstruct the despeckled image f .

G. Total Variation Filter

It is observed that the noise will be at high frequencies and the signals and images with excessive & spurious detail will have the high total variation i.e. the integral of the absolute gradient of those signals and images is high. Based on these observations it is proposed to reduce the total variation of the signal or image subject to it for getting a close match to the original signal. This is the key idea behind the denoising using total variational method.

The total variational technique has advantages over the traditional de-noising methods such as linear smoothing, median filtering, Transform domain methods using Fast Fourier transform and Discrete Cosine Transform which will reduce the noise in medical images but also introduce certain amount of blur in the process of

denoising which will damage the texture in the images in lesser or greater extent. The Total Variational approach will remove the noise present in flat regions by simultaneously preserving the edges in the medical images which are very important in diagnostic stage [17].

2.11 WAVELETDOMIN NOISE FILTERING

2.11.1 Brief history

In 1807, theories of frequency analysis by Joseph Fourier were the main lead to wavelet. However, wavelet was first appeared in an appendix to the thesis of A. Haar in 1909.

Compact support was one property of the Haar wavelet which means that it vanishes outside of a finite interval. Unfortunately, Haar wavelets have some limits, because they are not continuously differentiable. In 1930, work done separately by scientists for representing the functions by using scale-varying basis functions was the key to understanding wavelets. In 1980, Grossman and Morlet, a physicist and an engineer, provided a way of thinking for wavelets based on physical intuition through defining wavelets in the context of quantum physics. In 1985, a jump-start was given to wavelets by Stephane Mallat through his work in digital signal processing. He discovered relationships between quadrature mirror filters, pyramid algorithms and orthonormal wavelets bases. Later, Ingrid Daubechies constructed a set of orthonormal basis functions which become the start of wavelet applications today.

The main idea that describes wavelets is simply, scaling can lead to analyzing. It depends on mathematical principles for dividing data into different frequency components, then studying every individual component according to its scale. The scale is very important factor in wavelet analysis, since wavelets process data at different scales and resolutions. High level features can be noticed if the signal is studied in large windows, than if it is studied in small one. However, the wavelet analysis goal is to see both high level features and low level features of the signals. Since sines and cosines have infinite limits, then they are very poor in approximating choppy signals. This forces the scientists to look for an alternative functions for this type of approximation. The answer was wavelets, which are very suitable for approximating sharp spikes.

The wavelet analysis starts with adopting a wavelet prototype function called the mother wavelet. The frequency analysis is carried out with a low frequency version

of the wavelet, while the temporal analysis is achieved with the high frequency version of the mother wavelet [18].

Recently there has been significant investigations in medical imaging area using the wavelet transform as a tool for improving medical images from noisy data. Wavelet de-noising attempts to remove the noise present in the signal while preserving the signal characteristics, regardless of its frequency content. As the discrete wavelet transform (DWT) corresponds to basis decomposition, it provides a non-redundant and unique representation of the signal. Several properties of the wavelet transform, which make the use of wavelet technique attractive for de-noising, are:

1. Multi-resolution - image details of different sizes are analyzed at the appropriate resolution scales
2. Sparsity - the majority of the wavelet coefficients are small in magnitude.
3. Edge detection - large wavelet coefficients coincide with image edges.
4. Edge clustering - the edge coefficients within each sub band tend to form spatially connected clusters.

During a decomposition of an image, the two-dimensional data is replaced with four blocks. These blocks correspond to the sub bands that represent either low pass filtering or high pass filtering in each direction [19].

2.11.2 Wavelet transforms

There are many different types of wavelets transform. Most of data analysis applications are using continuous-time wavelet transform (CWT). However, the most famous type which affected the properties of many real signals is discrete wavelet transform (DWT) [18].

In this research the highlight on the second type (DWT) which is used in the proposed technique.

2.11.3 DISCRETE WAVELET TRANSFORM

A discrete wavelet transform represents a time domain signal into time frequency domain and the signals are called wavelet coefficients.

To ensure that high and low frequencies disturbance are extracted, two scale signal decomposition are performed. The wavelet transform output consists of two decomposed signals, with different levels of resolution. The range of frequencies

for the first and second scaled signal are $(f/2-f/4)$ and $(f/4-f/8)$ respectively, where f is the sampling frequency of the time domain signal.

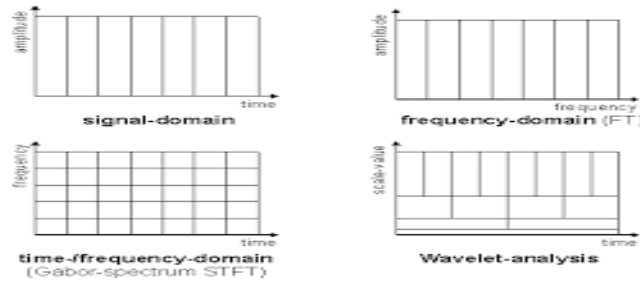


Figure 2.4: show the wavelet analysis [20].

2.11.4 Wavelet Decomposition

Originally known as optimal sub-band tree structuring (SB-TS) also called wavelet packet decomposition (WPD), is a wavelet transform where the discrete-time (sampled) signal is passed through more filters than the discrete wavelet transform (DWT).

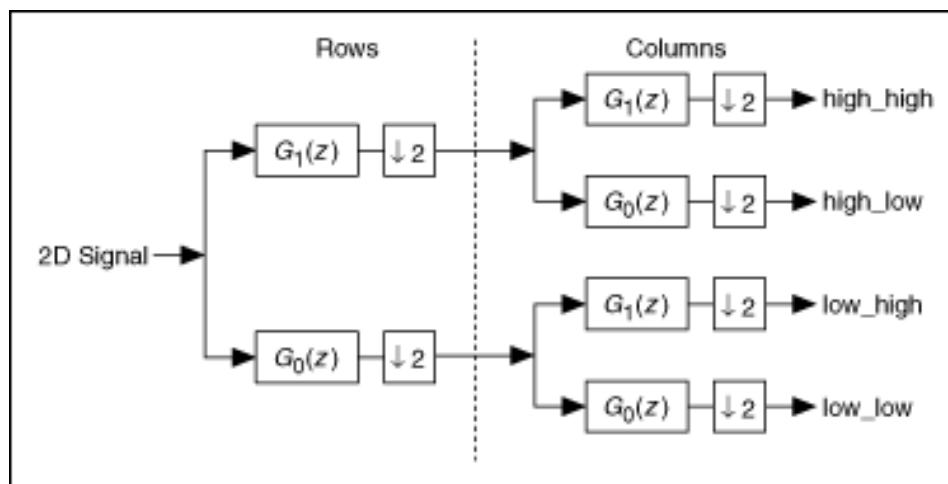


Figure 2.5: show the 2D wavelet decomposition [21].

The wavelet decomposition results in levels of approximated and detailed coefficients.

The 2-D DWT operates in a straightforward manner by inserting array transposition between the two dimensional Discrete Wavelet Transform. The rows

of the array are processed first with only one level of decomposition. This essentially divides the array into two vertical halves, with:

- i. The first half storing the average coefficients,
- ii. While the second vertical half stores the detail coefficients.

The noise is mainly appeared in the details.

This process is repeated again with the columns, resulting in four sub-bands. and is decomposed into four quadrants with different interpretations. Human visual system is very much sensitive to low frequency and hence, the decompose data available in the lower sub-band region and is selected and transmitted, information in the higher sub-bands regions are rejected depending upon required information content.

This multi-resolution analysis enables to analyze the signal in different frequency bands; therefore, we could observe any transient in time domain as well as in frequency domain [3].

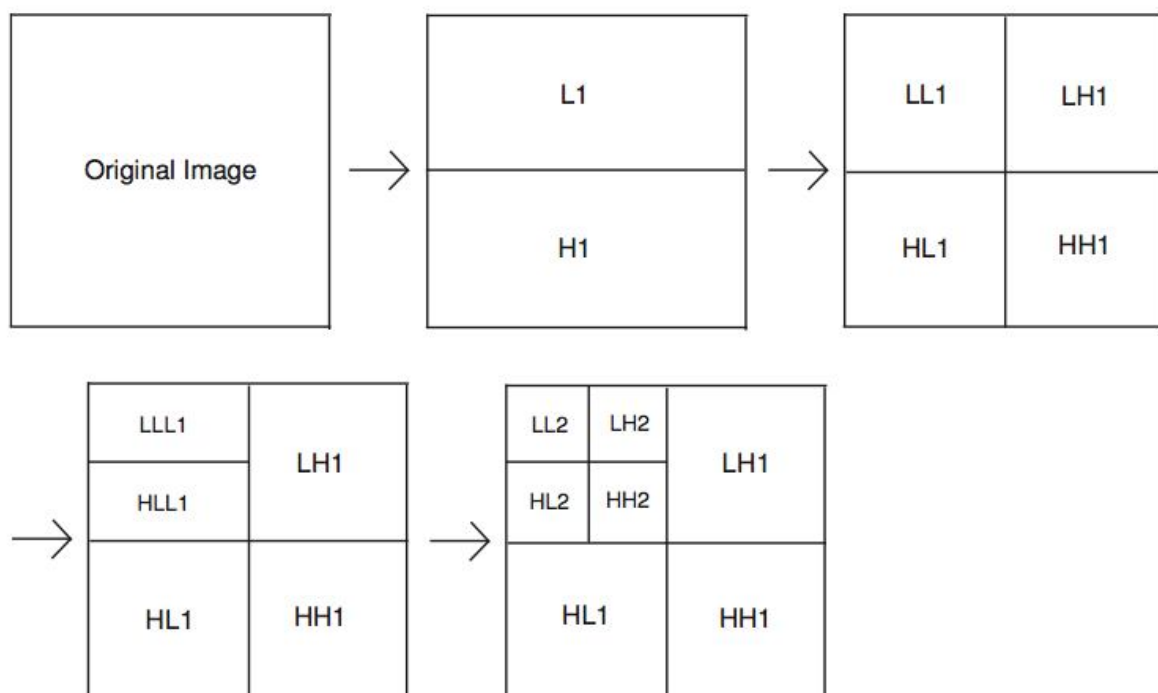


Figure 2.6: shows the sub-bands after the decomposition [22].

LL: The upper left quadrant consists of all coefficients, which were filtered by the analysis low pass filter h along the rows and then filtered along the corresponding

columns with the analysis low pass filter h again. This sub block is denoted by LL and represents the approximated version of the original at half the resolution.

HL/LH: The lower left and the upper right blocks were filtered along the rows and columns with h and g , alternatively. The LH block contains vertical edges, mostly. In contrast, the HL block shows horizontal edges very clearly.

HH: The lower right quadrant was derived analogously to the upper left quadrant but with the use of the analysis high pass filter g which belongs to the given wavelet. We can interpret this block as the area, where we find edges of the original image in diagonal direction [3].

The basic Procedure for all thresholding method is as follows:

- i. Calculate the DWT of the image.
- ii. Threshold the wavelet coefficients. (Threshold may be universal or sub band adaptive)
- iii. Compute the IDWT to get the de-noised estimate.

There are two thresholding functions frequently used, i.e. a hard threshold, a soft threshold.

The hard-thresholding is described as:

$$\eta_1(w) = wI(|w| > T) \quad (2.8)$$

Where w is a wavelet coefficient, T is the threshold.

The soft-thresholding function is described as:

$$\eta_2(w) = (w - \text{sgn}(w) T) I(|w| > T) \quad (2.9)$$

Where $\text{sgn}(x)$ is the sign function of x . The soft-thresholding rule is chosen over hard-thresholding [19].

As for as speckle (multiplicative nature)removal is concerned a preprocessing step consisting of a logarithmic transform is performed to separate the noise from the original image. Then different wavelet shrinkage approaches are employed. The different methods of wavelet threshold de-noising differ only in the selection of the threshold.

Wavelet Reconstruction

In practical, we often want to get its multi-stage reconstruction for a small wave, so that we can have a more accurate analysis of wavelet.

In wavelet analysis, when a signal or graphicsdecomposition, we need restore it and know that if we can get the original signal or graphics, so we need introduce the wavelet multistage reconstruction [23].

The figure below shows a multi-stage reconstruction process, In the figure, ‘h’ is low-pass filter, ‘g’ is high-pass filter, ‘ $\uparrow 2$ ’ is up sampling.

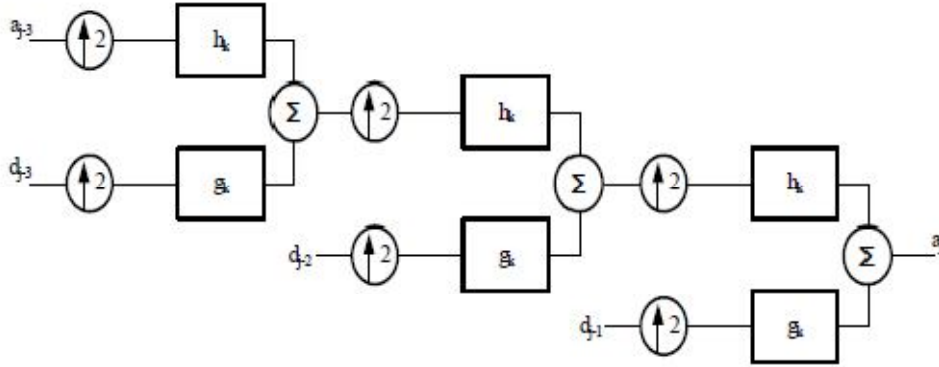


Figure (2.7): shows multi-stage reconstruction [23].

2.12Image quality assessment

Image quality is important when evaluating or segmenting ultrasound images, where speckle obscures subtle details in the image. In a recent study it is shown that speckle reduction improves the visual perception of the expert in the assessment of ultrasound imaging of the human organs. The statistical parameters like Signal to Noise Ratio (SNR), Mean Square Error (MSE) and Peak Signal to Noise Ratio (PSNR) for image quality assessment were used to evaluate the results.

2.12.1 RMSE

Root mean squared error

RMSE is an estimator in many ways to quantify the amount by which a filtered/noisy image differs from noiseless image. Andis the squared error averaged over an $M \times N$ window:

$$RMSE = \sqrt{\frac{1}{MN} \sum_{i=1}^M \sum_{j=1}^N (g_{i,j} - f_{i,j})^2} \quad (2.10)$$

2.12.2 SNR

Signal to Noise Ratio

The SNR compares the level of desired signal to the level of background noise. The higher the ratio, the less obtrusive the background noise is. It is expressed in decibels (dB) as

$$SNR = 10 \log_{10} \frac{\sum_{i=1}^M \sum_{j=1}^N (g_{i,j}^2 + f_{i,j}^2)}{\sum_{i=1}^M \sum_{j=1}^N (g_{i,j} - f_{i,j})^2}. \quad (2.11)$$

2.12.3 PSNR

Peak Signal to Noise Ratio

PSNR is the ratio between possible power of a signal and the power of corrupting noise that affects the fidelity of its representation.

$$PSNR = -10 \log_{10} \frac{MSE}{g_{\max}^2}, \quad (2.12)$$

The PSNR is higher for a good quality image and lower for a poor quality image. It measures image fidelity, that is, how closely the transformed image resembles the original image.

Chapter Three

Literature review

Speckle noise becomes a dominating factor in degrading the image visual quality and perception in medical images.

Before using ultrasound, the very first step is to reduce the effect of Speckle noise. Most of speckle reduction techniques have been studied by researchers; however there is no comprehensive method that takes all the constraints into consideration. This chapter adduces an overview about the previous studies and various techniques that has been used in the speckle noise reduction domain:

Jyotijaybhay and RajveerShastri,**a study of speckle noise education filters**(June 2015),Different filters have been developed as Mean and Median filters, SRAD filter.This paper reviews filters which are used to remove speckle noise.

NishthaAtlas *, Dr. Sheifali Gupta **,**Reduction of Speckle Noise in Ultrasound Images using Various Filtering techniques and Discrete Wavelet Transform: Comparative Analysis** (July 2014).This paper presents study of various techniques for removal of speckle noise from biomedical images such as Spatial and frequency domain filter and a modified algorithm for speckle noise reduction using wavelet based Multiresolutional analysis and combined filtering techniques with wiener and median filters. A comparative analysis of three methods: DWT with wiener filtering, DWT with median filtering and DWT with both wiener and median filtering techniques have been presented. Results are compared in terms of PSNR, Mean squared Error and processing time.

Radek BENES1, Kamil RIHA1,**MEDICAL IMAGE DENOISING BY IMPROVED KUAN FILTER** (2012 | MARCH).This paper focuses on the issue of speckle noise and its suppression. Firstly, the multiplicative speckle noise model and its mathematical formulation are introduced. Then, certain de-noising methods are described together with possible improvements. On their basis, an improvement of Kuan method (KuanS) is proposed. Performance of proposed KuanS method is tested on real ultrasound images and synthetic images corrupted with speckle noise.

Dr.T.Saravanan, HOD, ETC Department, Bharath University,NOISE REMOVAL IN ULTRASOUND IMAGES (*April 2012*).This paper presents the noise cleaning of biomedical ultrasonic images and its VLSI implementation. An optimized architecture has been designed with proper parallelism and pipelining as well as removing redundancies. In Ultrasound Images the quality of image is degraded by a special type of acoustic noise known as speckle noise. This is

reduces the ability of human observer to fetch important information from the image by masking the low contrast portions of the same, and this is multiplicative in nature. This noise can be removed through the homomorphic filter. The proposed method reduces the functional complexity when compared to the existing method. The VLSI implementation is done using modelsim 6.3 and xilinx 12.3.

Kamalpreet Kaur¹, Baljit Singh² and Mandeep Kaur³, **SPECKLE NOISE REDUCTION USING 2-D FFT IN ULTRASOUND IMAGES (Sept 2012)**. This paper presents a 2-D FFT removal algorithm for reducing the speckle noise in ultrasound images. We apply the 2-D FFT on the ultrasound images to extract and remove the peaks which are corresponding to speckle noise in the frequency domain. The performance of the proposed method is tested on ultrasound images.

T.RathaJeyalakshmi and K.Ramar, **A Modified Method for Speckle Noise Removal in Ultrasound Medical Images (February,2010)**, this paper describes and analyses an algorithm for cleaning speckle noise in ultrasound medical images. Mathematical Morphological operations are used in this algorithm. This algorithm is based on Morphological Image Cleaning algorithm (MIC) designed by Richard Alan Peters II. The algorithm uses a different technique for reconstructing the features that are lost while removing the noise. For morphological operations it also uses arbitrary structuring elements suitable for the ultrasound images which have speckle noise.

Raman Maini and Himanshu Aggarwal, **A Novel Technique for Speckle Noise Reduction on Medical Images (2010)**, In this paper, a new filter has been proposed which works by passing an image through a filter which works by raising pixels that are darker than their surrounding neighbors, then complementarily lowering pixels that are brighter than their surrounding neighbors to reduce the speckle index of that image. The proposed method has been compared with mean, median, Local Region Filter, Lee and Diffusion Filter using quantitative parameters like MSE and SNR. It has been found that the proposed method performs better than all other methods while still retaining the structural details.

Laurence Aroquiaraj^{1*}, K. Thangavel¹, R. Manavalan², **Comparative Analysis of Speckle Filtering Techniques (November 2009)**, the removal of speckle noise in ultrasound medical image is still a challenging one in medical image processing and analysis. Since, there is no common filter for speckle reduction. In this paper, we proposed six nonlinear techniques with combiner approach for image filtering

especially for speckle removal task, viz., MNHP Filter, ANHP Filter, TNHP Filter, MMNHP Filter, AMNHP Filter and TMNHP Filter. The proposed filters are evaluated and compared to achieve using their performance on ultrasound breast cancer images.

Yong Yue, *Student Member, IEEE*, Mihai M. Croitoru, Akhil Bidani, Joseph B. Zwischenberger, and John W. Clark, Jr., *Fellow, IEEE*, **Nonlinear Multiscale Wavelet Diffusion for Speckle Suppression and Edge Enhancement in Ultrasound Images (March 2006)**, This paper introduces a novel nonlinear multiscale wavelet diffusion method for ultrasound speckle suppression and edge enhancement. This method is designed to utilize the favorable denoising properties of two frequently used techniques: the sparsity and multiresolution properties of the wavelet, and the iterative edge enhancement feature of nonlinear diffusion. With fully exploited knowledge of speckle image models, the edges of images are detected using normalized wavelet modulus. Relying on this feature, both the envelope-detected speckle image and the log-compressed ultrasonic image can be directly processed by the algorithm without need for additional preprocessing. Speckle is suppressed by employing the iterative multiscale diffusion on the wavelet coefficients. With a tuning diffusion threshold strategy, the proposed method can improve the image quality for both visualization and auto-segmentation applications. We validate our method using synthetic speckle images and real ultrasonic images. Performance improvement over other despeckling filters is quantified in terms of noise suppression and edge preservation indices.

Karl Krissian, Kirby Vosburgh, Ron Kikinis and Carl-Fredrik Westin, **Anisotropic Diffusion of Ultrasound Constrained by Speckle Noise Model (October 2004)**. In this work, we propose to extend the current anisotropic diffusion technique to deal with the speckle noise present in the Ultrasound images. To this end, we use a previously derived model of the noise, and we write the restoration scheme as an energy minimization constrained by the noise model and parameters. This approach leads to a new data attachment term whose optimal weight can be automatically estimated.

Khaled Z. Abd-Elmoniem, *Student Member, IEEE*, Abou-Bakr M. Youssef, and Yasser M. Kadah*, *Member, IEEE*, **Real-Time Speckle Reduction and Coherence Enhancement in Ultrasound Imaging via Nonlinear Anisotropic Diffusion (SEPTEMBER 2002)**, This paper presents a novel approach for speckle reduction and coherence enhancement of ultrasound images based on nonlinear coherent diffusion (NCD) model. The proposed NCD model combines three different models. According to speckle extent and image anisotropy, the NCD

model changes progressively from isotropic diffusion through anisotropic coherent diffusion to, finally, mean curvature motion. This structure maximally low-pass filters those parts of the image that correspond to fully developed speckle, while substantially preserving information associated with resolved-object structures. The proposed implementation algorithm utilizes an efficient discretization scheme that allows for real-time implementation on commercial systems. The theory and implementation of the new technique are presented and verified using phantom and clinical ultrasound images. In addition, the results from previous techniques are compared with the new method to demonstrate its performance.

MR. HITESH S. ASARI, 2ASS.PROF. AMI SHAH, **A Research Paper on Reduction of Speckle Noise In Ultrasound Imaging Using Wavelet And Contourlet Transform.** In this paper, speckle noise removed is done by methods based on wavelet transform and contourlet transform. The two proposed alternative methods are evaluated and compared in terms of filter assessment parameters namely peak Signal to Noise Ratio (PSNR), Signal to Noise Ratio (SNR), Mean Square Error (MSE), Variance and Correlation Coefficient (CC). At last this method compare wavelet and counterlet transforms and see which better transform is.

FaouziBenzarti, Hamid Amiri,**Speckle Noise Reduction in Medical Ultrasound Images.**In this paper, we propose a de-noising approach which combines logarithmic transformation and a nonlinear diffusion tensor. Since speckle noise is multiplicative and nonwhite process, the logarithmic transformation is a reasonable choice to convert signal dependent or pure multiplicative noise to an additive one. The key idea from using diffusion tensor is to adapt the flow diffusion towards the local orientation by applying anisotropic diffusion along the coherent structure direction of interesting features in the image. To illustrate the effective performance of our algorithm, we present some experimental results on synthetically and real echo graphic images.

NouraAzzabou,and Nikos Paragios ,**SPATIO-TEMPORAL SPECKLE REDUCTION IN ULTRASOUND SEQUENCES.** In this paper they propose a novel variational framework for speckle removal in ultrasound images. Their method combines efficiently a fidelity to data term adapted to the Rayleigh distribution of the speckle and a novel spatio- temporal smoothness constraint. The regularization relies on Non parametric image models that describes the observed image structure and express inter-dependencies between pixels in space and time. The interaction between pixels is determined through the definition of new measure of similarity between them to better reflect image content. To compute

this similarity measure, we take into consideration the spatial aspect as well as the temporal one. Experiments were carried on both synthetic and real data and the results show the potential of our method.

R.VANITHAMANI¹, G.UMAMAHESWARI², M.EZHILARASI³,**Modified Hybrid Median Filter for Effective Speckle Reduction in Ultrasound Images.**This paper proposes a statistical filter, which is a modified version of Hybrid Median Filter for speckle reduction, which computes the median of the diagonal elements and maximum of the horizontal and vertical elements in a moving window and finally the two values are compared with the central pixel and the median value of the three values will be the new pixel value. The filter is tested on phantom Ultrasound image. Effectiveness of the proposed filter is compared on the basis of Peak Signal to Noise Ratio (PSNR), Root Mean Square Error (RMSE), Structure Similarity Index (SSI), Image Quality Index (QI) and Edge Preservation Factor (EPF) .The experimental results demonstrate that the proposed filter can reduce the speckle noise effectively without blurring the edges.

Chapter four

Materials and Methodology

Ten different filtering methods were applied on **three** ultrasound images (liver, fetal and abnormal GYN) with two levels of multiplicative noise (variances $\sigma_n = 0.5$, $\sigma_n = 0.05$). The image has been acquired from the Children's Hospital of Philadelphia database of fetal ultrasound images, and IBE Tech (Giza. Egypt) database of ultrasound images including liver and abnormal GYN, in JPG format.

This chapter explains the materials and the steps of the hybrid technique which is an improvement of the result that can be obtain using each filter individually, so the quality of the process increase and it is better for preserving the image texture.

4.1 The proposed method

(Hybrid technique)

The research describes a hybrid technique for reducing such speckle noise. This algorithm is based on wavelet decomposition (first level) in combination with two filters (SRAD and hybrid median filter). The discrete wavelet decomposition (DWT) works by analyzing the images using wavelet decomposition, which is produced 4-sub bands (LL, LH, HL, and HH).

In this technique the LL subband was de-noised by SRAD filter which is works without losing texture information .the noise in the three high frequency subbands were extracted from the texture by hybrid median filter,and then the image reconstructed using the inverse discrete wavelet transform(IDWT), for more finesse the resulted image was passed through a total variation filter for the second time to get better enhancement.

The proposed method algorithm:

step1: Calculate the DWT of the image (decomposition).

Step2: Apply the SRAD filter on the LL sub band.

Step3: Apply the hybrid median filter on the three higher sub-bands (LH, HL and HH).

Step4: Compute the IDWT to get the reconstructed image.

Step5: Passes the reconstructed image through a total variation filter.

Step6: Calculate the IMQs values to evaluate the final image.

The reasons behind using these filters, it's to make a maximum benefit from the advantages and characteristics of each one by combining them in a novel fashion.

These characteristics are:

Improving the result of later processing by removing noise from the signal and additionally preserves the edges, that is for the hybrid median filter.

Eliminating speckle without distorting useful image information and without destroying the important image edge, that is for the SRAD filter.

The Total Variational approach will remove the noise present in flat regions by simultaneously preserving the edges in the medical images which are very important in diagnostic stage.

4.2 The proposed method flow chart

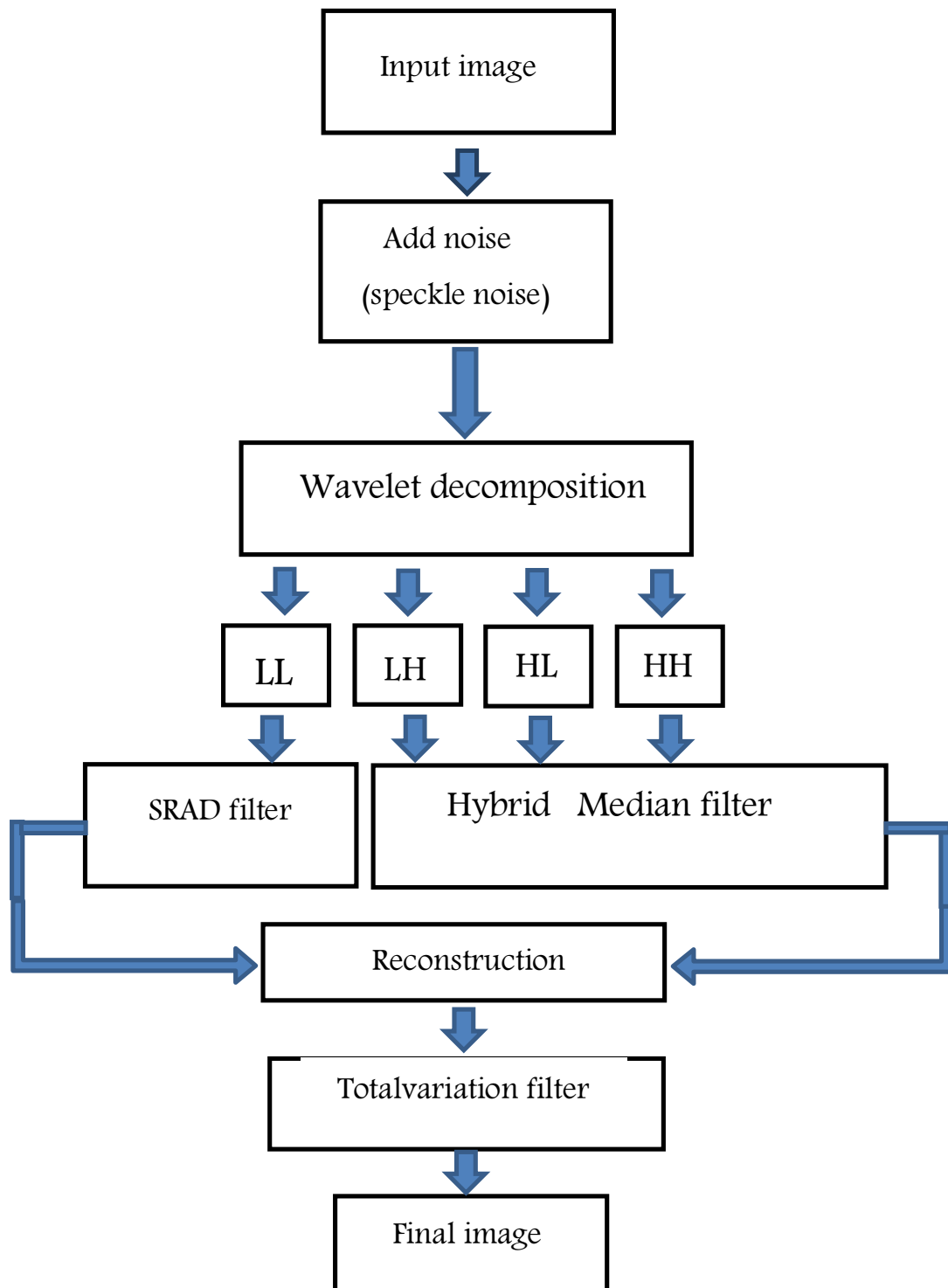


Figure 4.1: show the flow chart of the proposed method.

Chapter five

Results and Discussions

5.1 Experimental Results

Ten different filtering methods were applied on **three** ultrasound images (liver, fetal and abnormal GYN) with two levels of multiplicative noise (variances $\sigma_n = 0.5$, $\sigma_n = 0.05$). The image has been acquired from the Children's Hospital of Philadelphia database of fetal ultrasound images, and IBE Tech (Giza. Egypt) database of ultrasound images including liver and abnormal GYN, in JPG format.

To estimate the performance of the proposed technique, the **Ten** different filtering methods namely: Neighborhood averaging (DsFlecasort), First Order Statistics Filtering (DsFlsmv), Homogenous area (DsFlsminsc) linear scaling gray level filter(DsFca),the local statistics of the noise image(DsFls),median filter, Hybrid median(DsFmedian), Total variation, wavelet, and SRAD(DsFsrاد),have been implemented in the same US images with both variance values.

In this chapter the differences between the original and despeckled images were evaluated using image evaluation metrics .which are easy to compute and have clear physical meaning.

Root Mean Squared error (RMSE), Signal to Noise ratio (SNR) and Peak signal to noise ratio (PSNR).which have been calculated from the denoised images.

The SNR and PSNR are higher for a better transformed image and lower for a poorly transformed image, on the contrary in RMSE.

The test results of US B-scan images namely liver, fetal and abnormal GYN with two variance values of multiplication noise ($\sigma_n = 0.05$ and $\sigma_n = 0.5$) given in the figures below. Also the computational result were computed and recorded on the next tables.

Firstly, the resulted bands from wavelet decomposition are shown in the figures below -for each image with two variances.

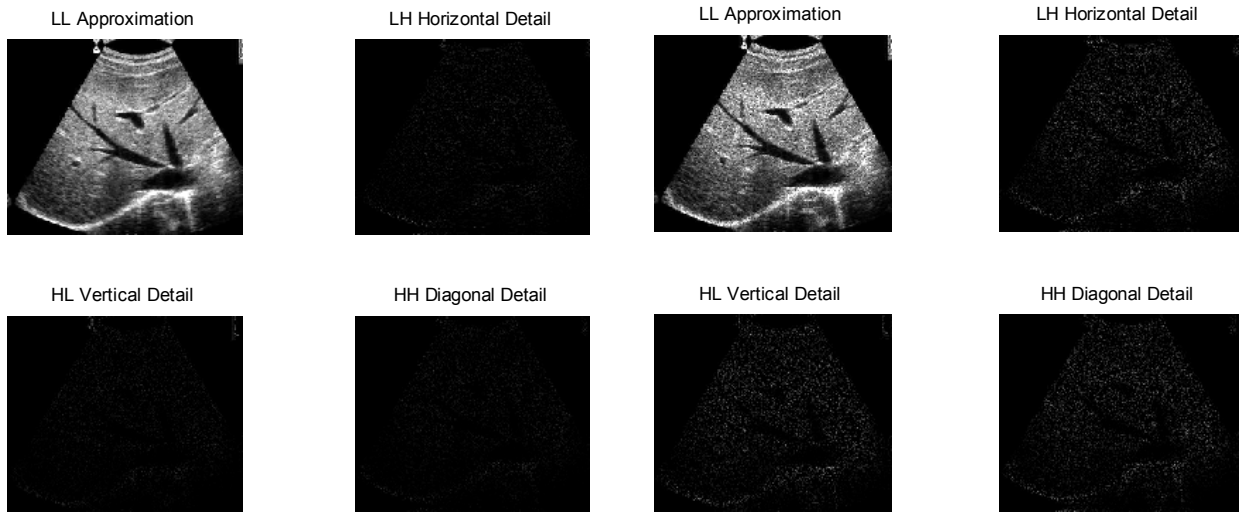


Figure 5.1: wavelet decomposition of the liver image with noise $\sigma_n = 0.05$ and $\sigma_n = 0.5$, respectively.

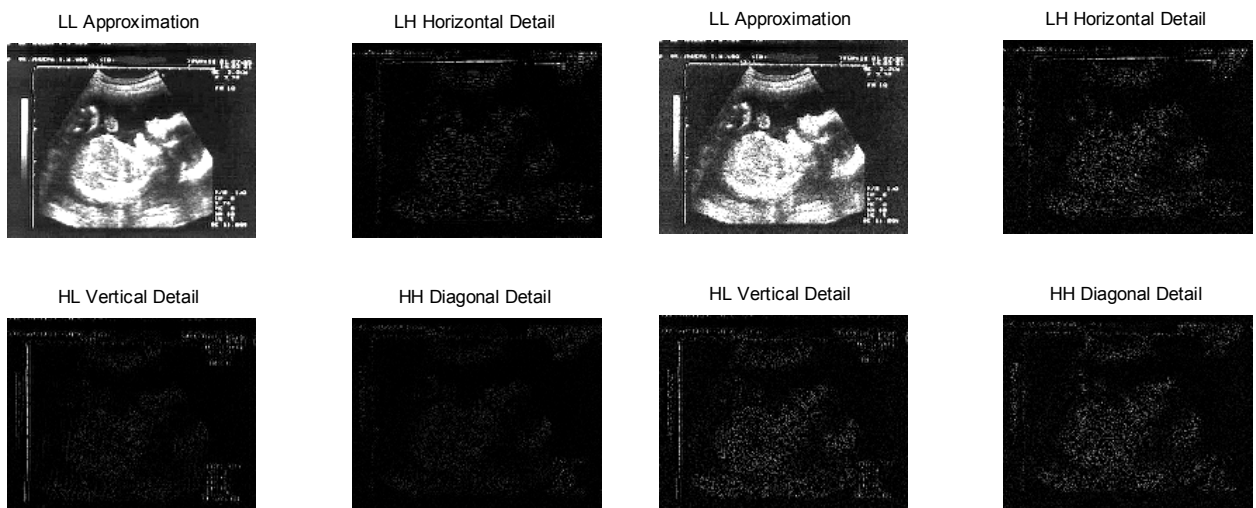


Figure 5.2: wavelet decomposition of the fetal image with noise $\sigma_n = 0.05$ and $\sigma_n = 0.5$, respectively

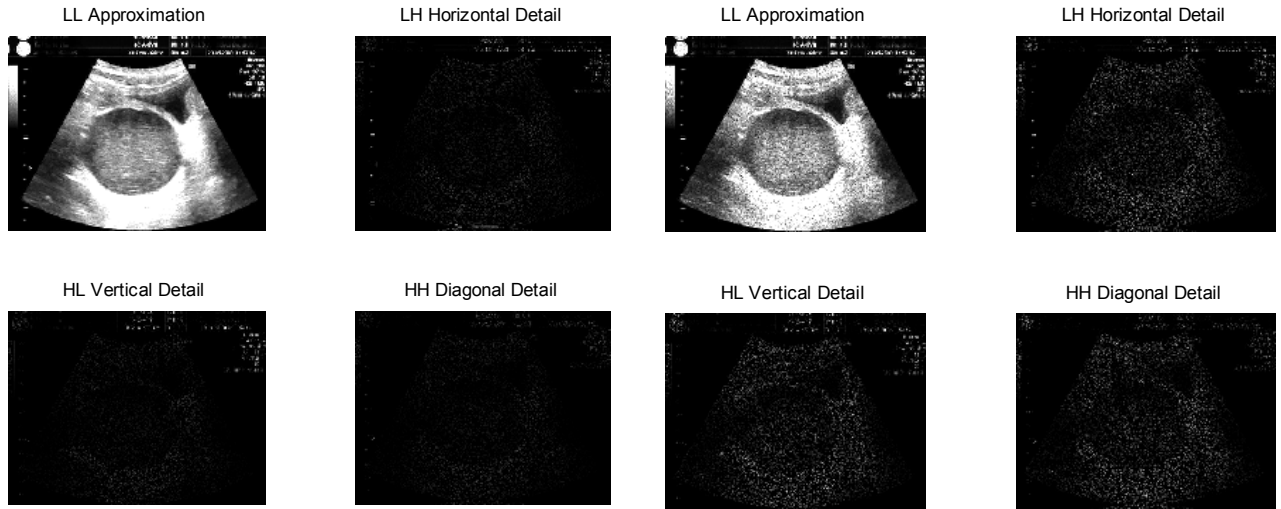
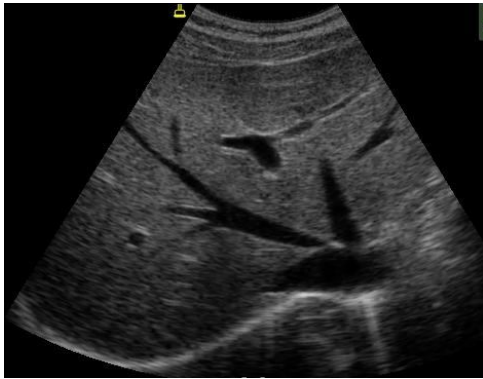


Figure 5.3: wavelet decomposition of the abnormal GYN image with noise $\sigma_n=0.05$ and $\sigma_n=0.5$, respectively.

Above figures 5.1,5.2 and 5.3 shows the low frequency subband LL and the high frequency subbands of horizontal,vertical and diagonal directions, respectively.

We can observe that most of the noise and texture are concentrated in the three high frequency subbands.

In this proposed method the LL subband was de-noised by SRAD filter which is works without losing texture information .the noise in the three high frequency subbands were extracted from the texture by hybrid median filter,and then the image reconstructed using the inverse discrete wavelet transform after that the resulted image was passed through a total variation filter for the second time to get better enhancement.



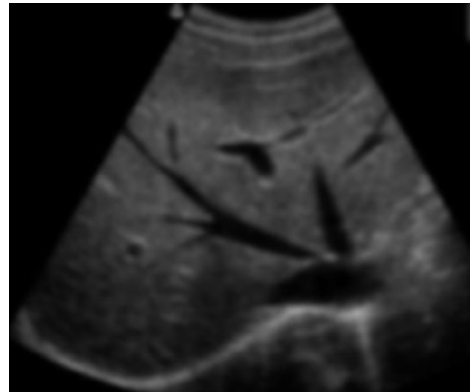
Original image



Noisy image



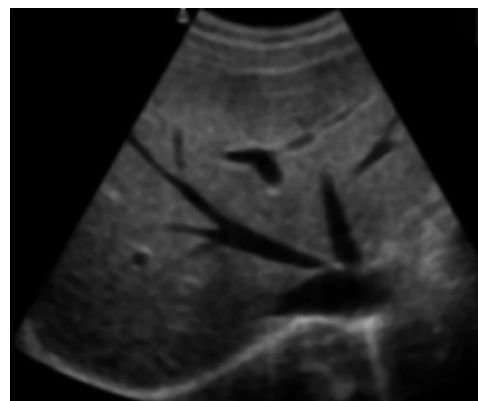
Linear scaling filtering



First Order Statistics Filtering



Local statistics filtering



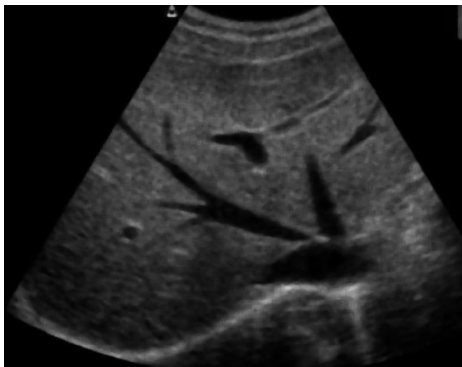
Neighborhood Averaging filter



Homogeneous Area Filtering



Total variation



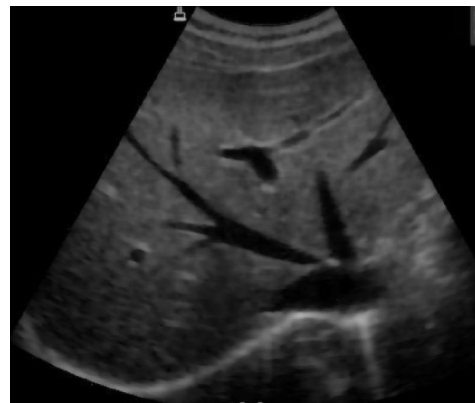
Normal median filter



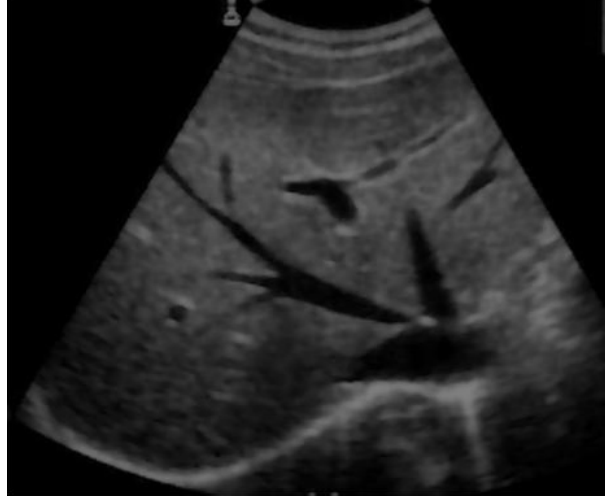
Wavelet filtering



Hybrid median filter



SRAD filter



Proposed method

Figure 5.4: results of liver image despeckled by various filters (variance $\sigma_n = 0.05$)

The Computational Results:

Table 5.1: the measures of image quality evaluation metrics is computed for the liver image (with variance $\sigma_n = 0.05$) at statistical measurement of RMSE, SNR and PSNR for different filter types and for the proposed method.

Filter	RMSE	SNR	PSNR
Neighborhood averaging filter (DsFlecasort)	45.3626	36.3903	38.9389
First order(DsFlsmv)	45.7977	36.5567	36.7934
Homogenous area (DsFlsminsc)	46.6122	36.6139	40.4238
Linear scaling (DsFca)	46.7710	36.8605	38.0074
Local statistics(DsFls)	46.6115	36.0307	38.2583
Normal median (med)	48.6119	36.8364	42.1102
Hybrid median(DsFmedian)	46.7674	36.6180	42.0074
Total variation	42.0761	36.6799	42.1102
Wavelet	48.2224	36.7708	42.7969
SRAD(DsFsrاد)	46.4168	36.6411	40.3823
Proposed method	43.0026	36.8703	42.2485

□ Bold number indicates the best result.

□ Root mean square error (RMSE), signal-to- noise ratio (SNR), peak signal-to- noise ratio (PSNR).

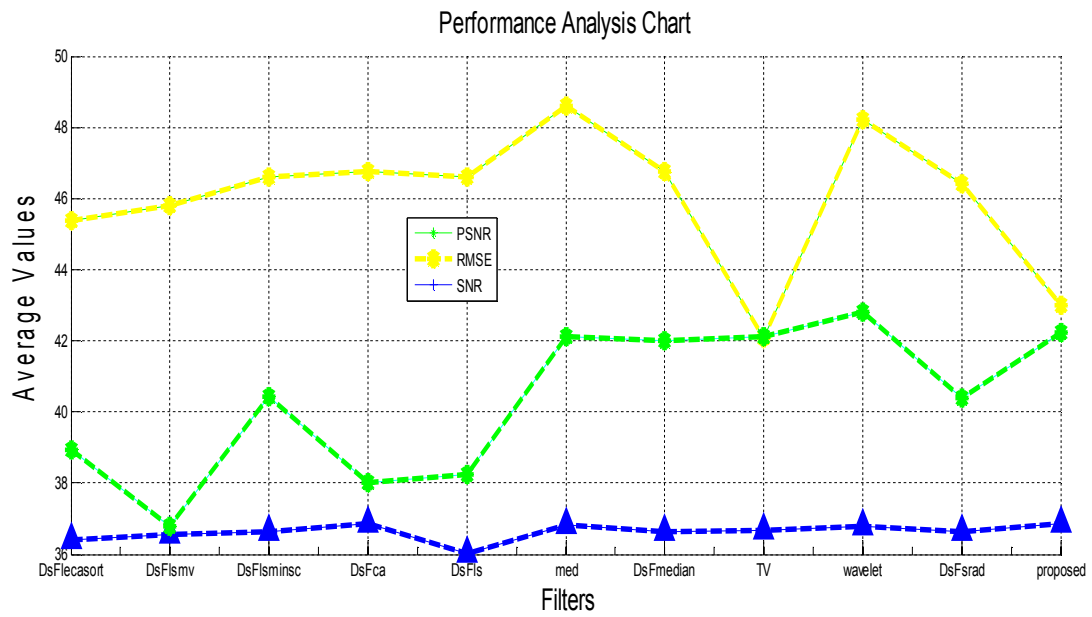
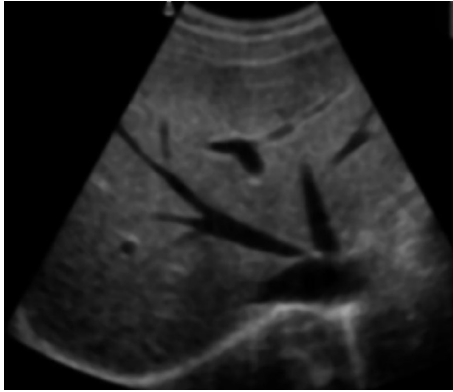


Figure 5.5: performance analysis graph for the computational results (IMQ) for the liver image ($\sigma_n = 0.05$)



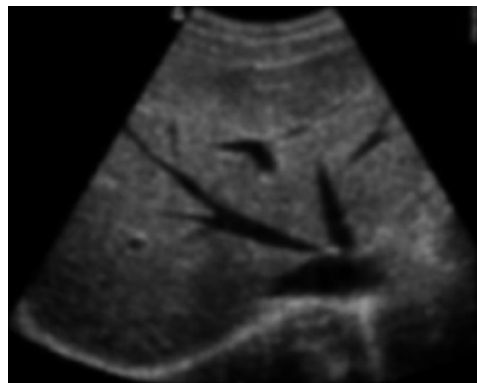
Original image



Noisy image



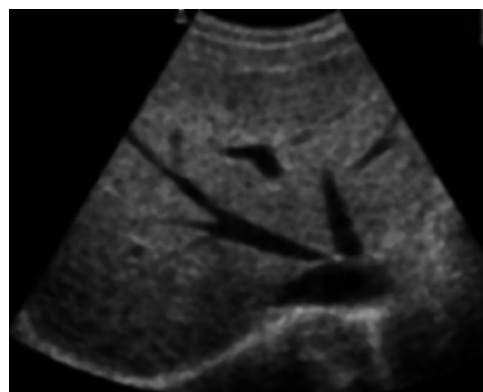
Linear scaling filtering



First Order Statistics Filtering



Local statistics filtering



Neighborhood Averaging filter



Homogeneous Area Filtering



Normal median filter



Hybrid median filter



Total variation



Wavelet filtering



SRAD filter



Proposed method

Figure 5.6: results of liver image despeckled by various filters (variance $\sigma_n = 0.5$)

The Computational Results:

Table 5.2: the measures of image quality evaluation metrics is computed for the liver image (with variance $\sigma_n = 0.5$) at statistical measurement of RMSE, SNR and PSNR for different filter types and for the proposed method.

Filter	RMSE	SNR	PSNR
Neighborhood averaging filter (DsFlecasort)	44.6821	36.2271	42.1102
First order(DsFlsmv)	45.8344	35.4904	36.5953
Homogenous area (DsFlsminsc)	47.0715	36.6534	41.2140
Linear scaling (DsFca)	50.2073	37.4118	41.1902
Local statistics(DsFls)	50.0653	37.2009	37.7138
Normal median (med)	57.8668	36.8425	40.0423
Hybrid median(DsFmedian)	49.5118	36.9030	41.4495
Total variation	52.3315	36.1022	41.8068
Wavelet	51.6483	37.0992	42.3713
SRAD(DsFsrاد)	46.4168	36.6411	40.3823
Proposed method	43.1194	37.2265	42.2761

□ Bold number indicates the best result.

□ Root mean square error (RMSE), signal-to- noise ratio (SNR), peak signal-to- noise ratio (PSNR).

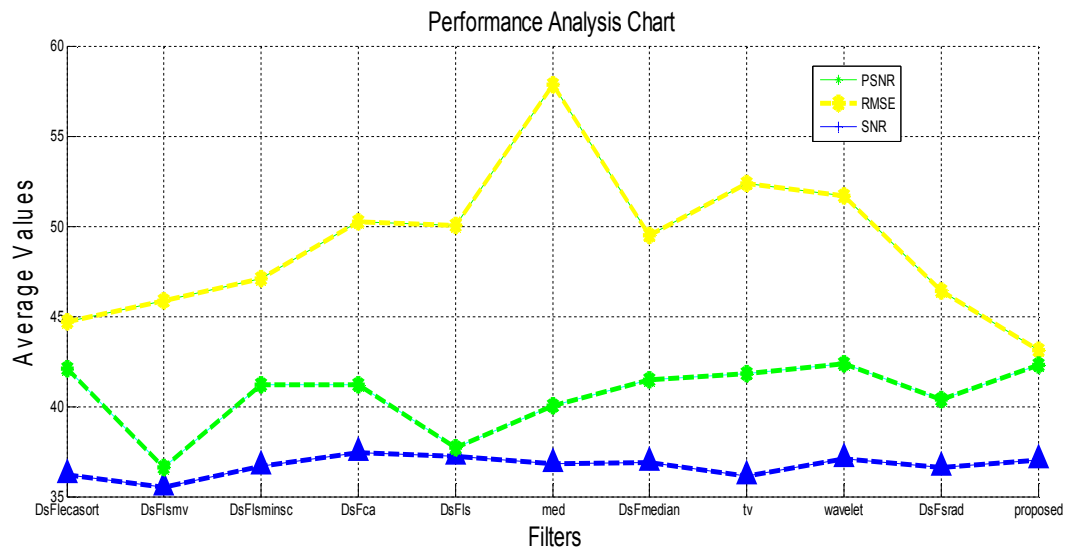


Figure 5.7: performance analysis graph for the computational results (IMQ) for liver image ($\sigma_n=0.5$)



Original image



Noisy image



Linear scaling filtering



Local statistics filtering



First Order Statistics Filtering



Neighborhood Averaging filter



Homogeneous Area Filtering



Normal median filter



Hybrid median filter



Total variation



Wavelet filtering



SRAD filter



The Computational Results:

Table 5.3: the measures of image quality evaluation metrics is computed for the fetal image (with variance $\sigma_n = 0.05$) at statistical measurement of RMSE, SNR and PSNR for different filter types and for the proposed method.

Filter	RMSE	SNR	PSNR
Neighborhood averaging (DsFlecasort)	74.4885	39.3541	41.5474
First order(DsFlsmv)	73.5968	39.5331	40.4651
Homogenous area (DsFlsminsc)	76.0977	39.6072	41.7981
Linear scaling (DsFca)	76.6039	40.1777	40.7086
Local statistics(DsFls)	76.0581	39.7801	40.1729
Normal median (med)	83.1476	40.2589	42.1103
Hybrid median(DsFmedian)	79.4809	39.9121	41.4495
Total variation	84.4204	40.1510	42.0031
Wavelet	82.8542	40.2119	42.1467
SRAD(DsFsrad)	80.7096	40.1086	41.1503
Proposed method	75.3745	39.9881	41.9864

□ Bold number indicates the best result.

□ Root mean square error (RMSE), signal-to- noise ratio (SNR), peak signal-to- noise ratio (PSNR).

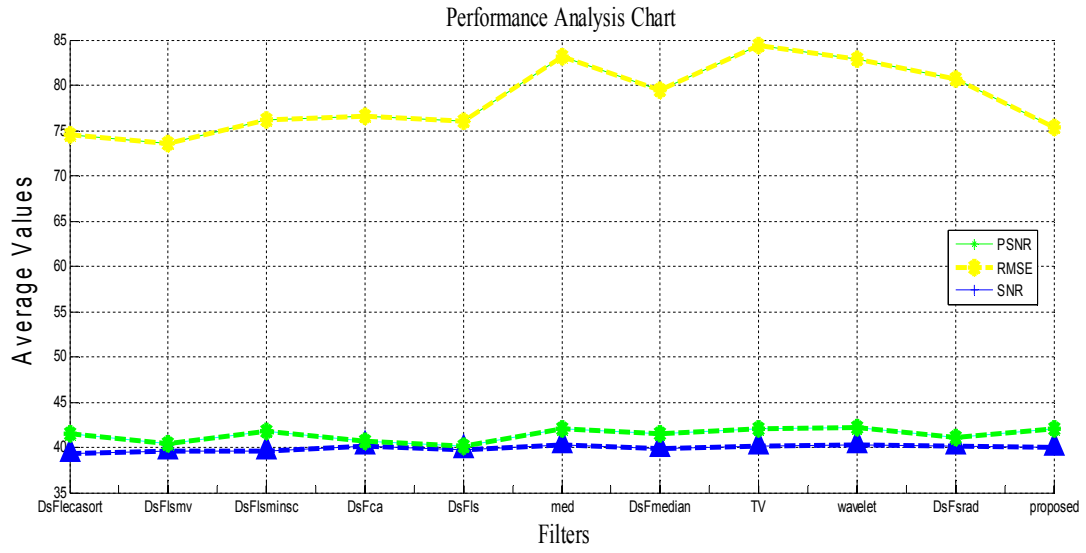


Figure 5.9: performance analysis graph for the computational results (IMQ) for the fetal image ($\sigma_n = 0.05$)



Original image



Noisy image



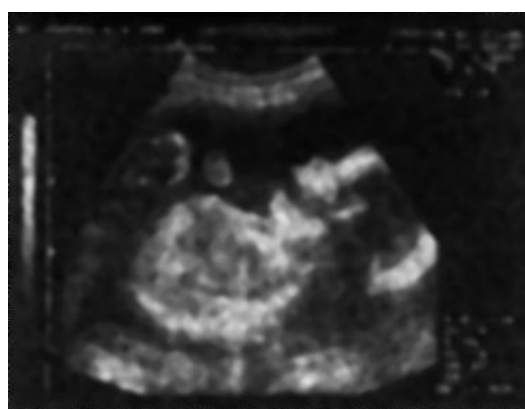
Linear Scaling Filtering



Local statistics filtering



First Order Statistics Filtering



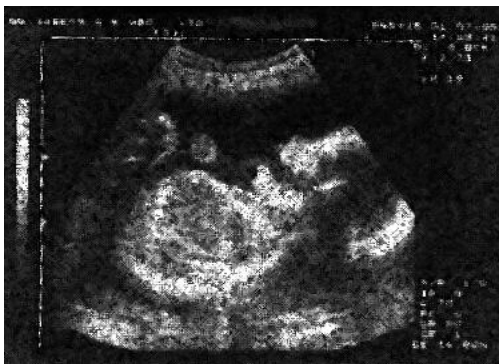
Neighborhood Averaging filter



Homogeneous Area Filtering



Normal median filter



Hybrid median filter



Total variation



Wavelet filtering



SRAD filter



Proposed method

Figure 5.10: results of fetal image despeckled by various filters (variance $\sigma_n = 0.5$)

The Computational Results:

Table 5.4: the measures of image quality evaluation metrics is computed for the fetal image (with variance $\sigma_n = 0.5$) at statistical measurement of RMSE, SNR and PSNR for different filter types and for the proposed method.

Filter	RMSE	SNR	PSNR
Neighborhood averaging (DsFlecasort)	73.2337	39.0676	40.0864
First order(DsFlsmv)	72.0380	39.3548	39.9808
Homogenous area (DsFlsminsc)	74.1848	40.3480	41.7981
Linear scaling (DsFca)	74.9701	37.3258	40.2126
Local statistics(DsFls)	74.6644	36.9022	40.2149
Normal median (med)	84.1541	40.2480	41.1253
Hybrid median(DsFmedian)	76.9851	39.5234	40.9579
Total variation	82.4473	39.9509	41.2781
Wavelet	83.9579	40.2359	42.1103
SRAD(DsFsrar)	80.7858	40.1001	42.1002
Proposed method	75.3785	40.5674	41.9381

□ Bold number indicates the best result.

□ Root mean square error (RMSE), signal-to- noise ratio (SNR), peak signal-to- noise ratio (PSNR).

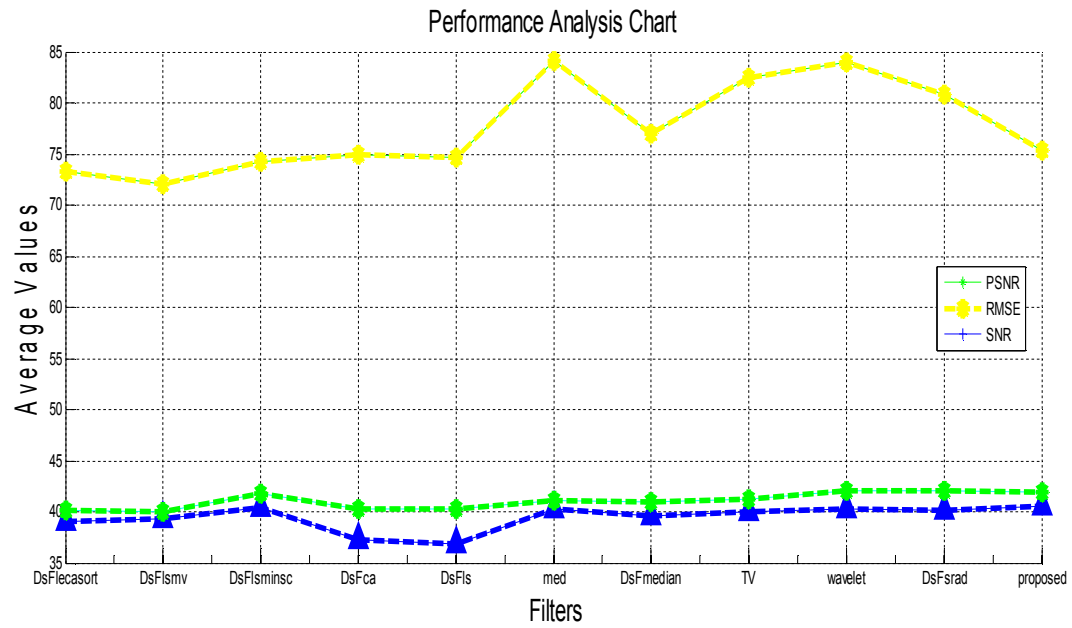
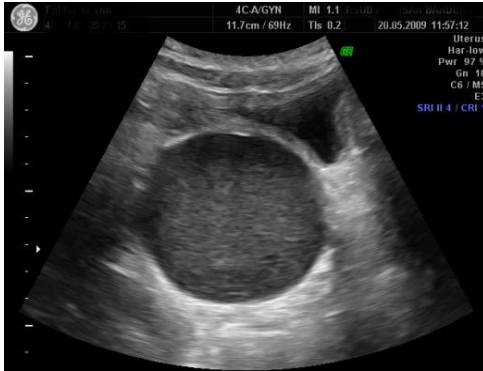


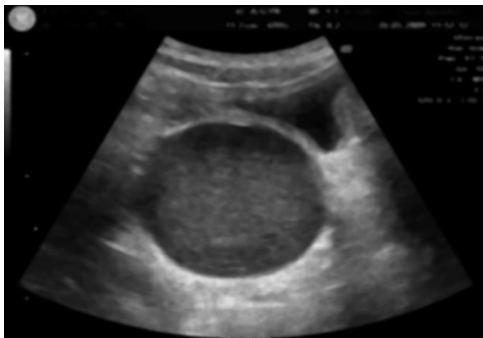
Figure 5.11: performance analysis graph for the computational results (IMQ) for fetal image ($\sigma_n = 0.5$)



Original image



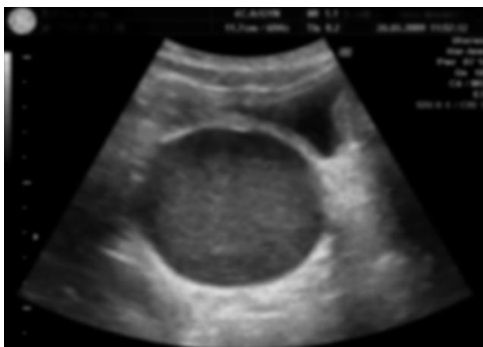
Noisy image



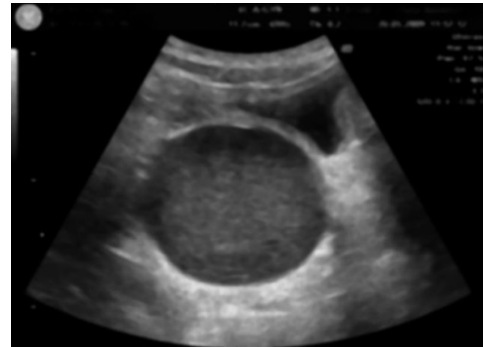
Linear scaling filtering



Local statistics filtering



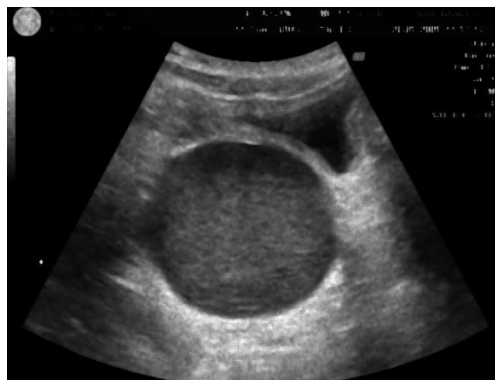
First Order Statistics Filtering



Neighborhood Averaging filter



Homogeneous Area Filtering



Normal median filter



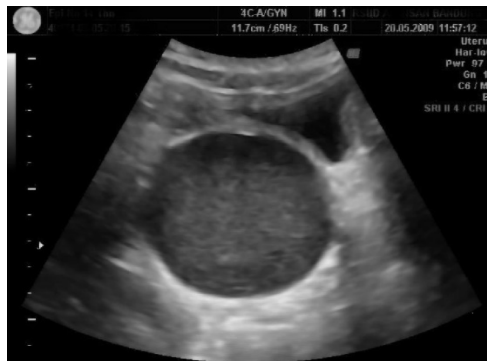
Hybrid median filter



Total variation



Wavelet filter



SRAD filter



Proposed method

Figure 5.12: results of abnormal GYN image despeckled by various filters (variance $\sigma_n = 0.05$)

The Computational Results:

Table 5.5: the measures of image quality evaluation metrics is computed for the abnormal GYN image (with variance $\sigma_n = 0.05$) at statistical measurement of RMSE, SNR and PSNR for different filter types and for

Filter	RMSE	SNR	PSNR
Neighborhood averaging (DsFlecasort)	61.9098	39.4557	41.0100
First order(DsFlsmv)	62.1435	39.5715	40.6685
Homogenous area (DsFlsminsc)	63.4000	39.6338	42.1033
Linear scaling (DsFca)	64.1164	39.8559	42.0002
Local statistics(DsFls)	63.6605	39.8294	39.6455
Normal median (med)	66.5610	39.8523	41.7603
Hybrid median(DsFmedian)	64.0782	39.6693	42.0952
Total variation	66.2238	39.8501	42.1103
Wavelet	67.1508	39.8669	42.1111
SRAD(DsFsrاد)	63.9915	39.7042	42.1102
Proposed method	62.0715	39.9863	42.2112

the proposed method.

□ Bold number indicates the best result.

□ Root mean square error (RMSE), signal-to- noise ratio (SNR), peak signal-to- noise ratio (PSNR).

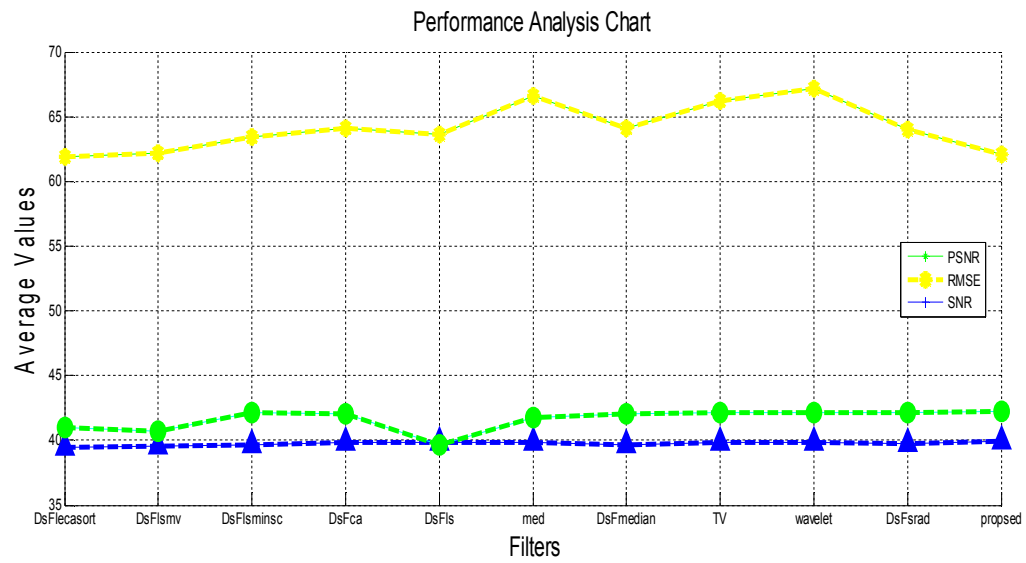
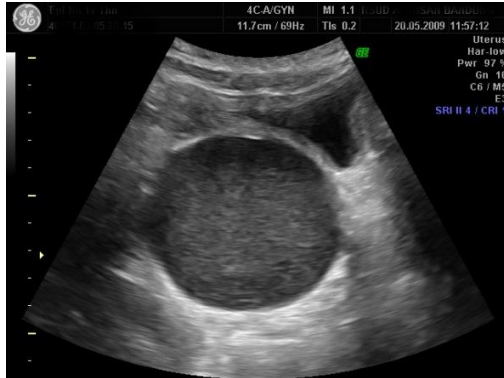
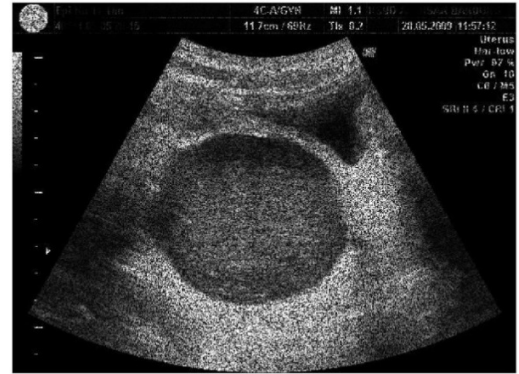


Figure 5.13: performance analysis graph for the computational results (IMQ) for the abnormal GYN image ($\sigma_n = 0.05$)



Original image



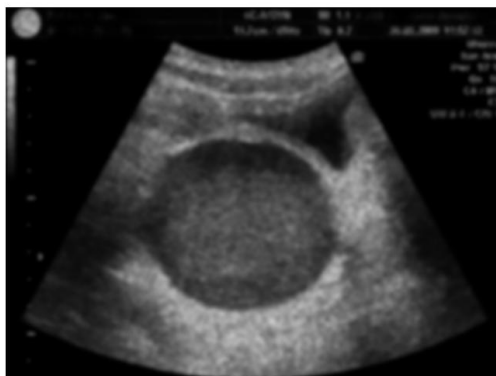
Noisy image



Linear scaling filter



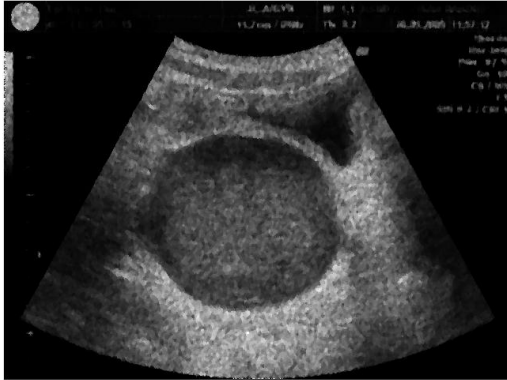
Local statistics filtering



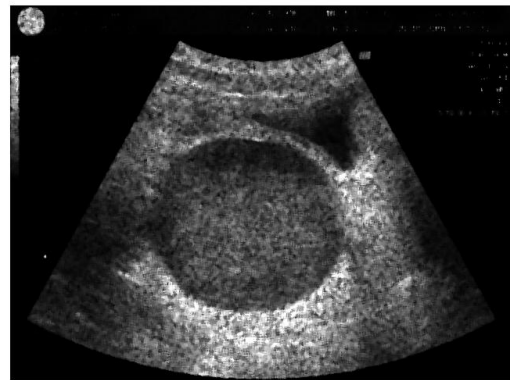
First Order Statistics Filtering



Neighborhood Averaging filter



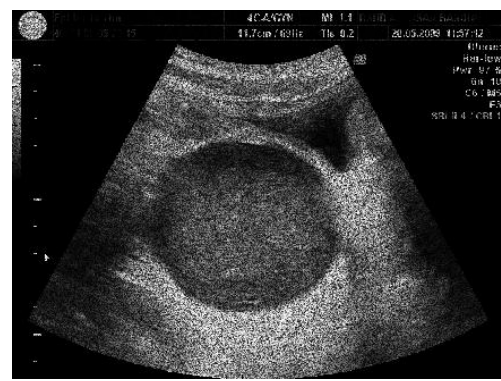
Homogeneous Area Filtering



Normal median filter



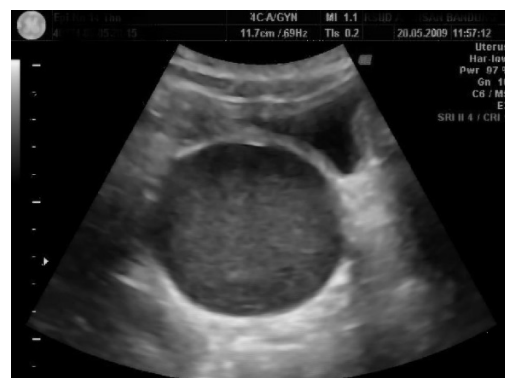
Hybrid median filter



Total variation



Wavelet filtering



SRAD filter



Proposed method

Figure 5.14: results of abnormal GYN image despeckled by various filters (variance $\sigma_n = 0.5$)

The Computational Results:

Table 5.6: the measures of image quality evaluation metrics is computed for the

Filter	RMSE	SNR	PSNR
Neighborhood averaging (DsFlecasort)	61.1489	39.3006	42.0100
First order(DsFlsmv)	61.5802	39.5402	39.0849
Homogenous area (DsFlsminsc)	63.0182	39.6023	42.1102
Linear scaling (DsFca)	63.6146	39.9751	42.2039
Local statistics(DsFls)	63.0811	39.9563	36.9638
Normal median (med)	76.0515	40.4285	42.1103
Hybrid median(DsFmedian)	67.1554	39.8165	41.3890
Total variation	70.6236	40.1171	42.0671
Wavelet	76.1046	40.4158	42.1103
SRAD(DsFsrاد)	63.9915	39.7042	42.0134
Proposed method	62.2062	39.9094	42.2302

abnormal GYN image (with variance $\sigma_n = 0.5$) at statistical measurement of RMSE, SNR and PSNR for different filter types and for the proposed method.

□ Bold number indicates the best result.

□ Root mean square error (RMSE), signal-to- noise ratio (SNR), peak signal-to- noise ratio (PSNR).

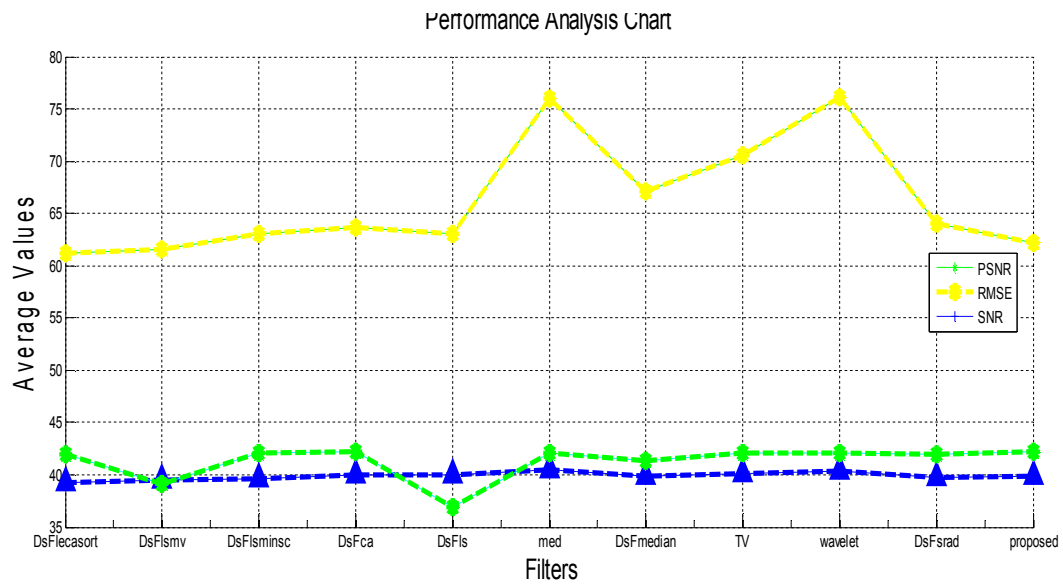


Figure 5.15: performance analysis graph for the computational results (IMQ) for abnormal GYN image ($\sigma_n=0.5$)

5.2 Discussion

Most importantly, more comparative studies of despeckle filtering are necessary for selecting the most appropriate filter or filters for the image under investigation.

The good Despeckle filter removes noise from images without blurring the image. It attempts to detect complex areas and leave these intact while smoothing areas where noise will be noticeable. While leaving complex areas untouched. The effect is that a noise is reduced without severely affecting edges.

In this research the proposed method have been builds on the ideas underlying three existing techniques, SRAD filtering, hybrid median filter and wavelet decomposition .but combines these ideas in a novel fashion.

The wavelet decomposition analyzes the image and represents a multi-resolution component (four subbands: LL, LH, HL, and HH), the LL band have been passed through the SRAD filter, it is work without affect the features of the object which is found in this band. And the higher frequency components (LH, HL and HH) were passed through a hybrid median filter which preserves the edges. For more optimization the total variation were applied on the reconstructed image.

Here we presented performance of the proposed method and compare our results with other conventional despeckling methods.

From the numeric values of RMSE, SNR and PSNR gave in the tables (5.1, 5.2, 5.3, 5.4, 5.5, and 5.6) and from figures (5.4, 5.6, 5.8, 5.10, 5.12 and 5.14) show the original images, noisy images and the despeckled images. It can be observed that the most of the despeckle filters has high degree of blurring and poor reduction of noise.

Although some of these filters perform well for removal of speckle noise, they have major limitations in preserving sharp features of the original image, whilst the proposed method give an acceptable improves in the quality of resultant images and performs better than other methods in saving the object features, giving good contrast and preserving the edges. For these reasons, the proposed method gives results better than using each of SRAD filter or hybrid median filter individually.

Chapter Six

Conclusion and Future Work

6.1 Conclusion

Among all modalities of medical imaging system, ultrasonography has been considered as one of the most non-invasive and powerful technique for imaging organs and soft-tissue structure of the human body. Ultrasonography is often preferred due to its relatively low-cost and also there are no ionizing radiations. Beside these advantages, medical ultra-sonographic images are of poor visibility, resulting from speckle noise.

Speckle noise is an inherent property of medical ultrasound imaging, and it generally tends to reduce the image resolution and contrast, thereby reducing the diagnostic value of this imaging modality. As a result, speckle noise reduction is an important prerequisite, whenever ultrasound imaging is used for tissue characterization. Many algorithms have been developed for despeckling.

In this research, we proposed a hybrid technique for reducing such speckle noise. This algorithm is based on wavelet decomposition (first level) in combination with two filters (SRAD and hybrid median filter).

A total of 10 different despeckle filters also were documented in this research based on linear filtering, nonlinear filtering, diffusion filtering and wavelet filtering. We have applied despeckle filtering on three ultrasound images of liver, fetal and abnormal GYN with two levels of variance values.

To test the efficiency of the filters mentioned above, the filters were applied to the noisy image. The performance of noise removing algorithms will be measured using quantitative performance measures such as RMSE, SNR and PSNR, which is known as Image quality metrics as well as in terms of visual quality of the images.

This study evaluates performances of each technique as well as the proposed method and demonstrates that, in most of these cases, the proposed method significantly improves the quality of resultant images and performs better than other methods. It can be observed from the numeric values of RMSE, SNR and PSNR, as well as visual evaluation.

6.2 Recommendations

1. For optimum result it can be used higher level of wavelet decomposition (2^{nd} level as example) before passing an image through the filter.
2. For the hybrid median filter it can be changed by modified hybrid median filter and for wavelet transform can be changed by the fast haar wavelet denosing.

Use Edge Preservation Factor (EPF) as one of the image quality evaluation metrics for accurate evaluation of the ability of filters in the edge preservation

References

References

1. R.Vanithamani and G.Umamaheswari, “ **Performance Analysis of Filters for Speckle Reduction in Medical Ultrasound Images** ”International Journal of Computer Applications (0975 – 8887) Volume 12– No.6, December 2010.
2. Laurence Aroquiaraj* , K. Thangavell and R. Manavalan,“**Comparative Analysis of Speckle Filtering Techniques**”, Department of Computer Science, Periyar University.
3. MR. HITESH S. ASARI, 2ASS.PROF. AMI SHAH,A.D. Patel institute and Technolagey, “ **A Research Paper On Reducion Of Speckle Noise In Ultrasound Imaging Using Wavelet And Contourlet Transform**”, JOURNAL OF INFORMATION, KNOWLEDGE AND RESEARCH IN ELECTRONICS ANDCOMMUNICATION ENGINEERING ISSN: 0975 – 6779| NOV 12 TO OCT 13 | VOLUME – 02, ISSUE - 02 Page 800.
4. Jens E. Wilhjelm, Andreas Illum, Martin Kristensson and Ole Trier Andersen, “**Medical diagnostic ultrasound- physical principles and imaging**”,Biomedical Engineering, DTU ElektroTechnical University of Denmark (Ver. 3.1, 2 October 2013) © 2001-2013 by J. E. Wilhjelm.
5. INSTITUTE OF PHYSICS PUBLISHING PHYSICS IN MEDICINE AND BIOLOGY, “**Ultrasound imaging**”, Phys. Med. Biol. **51** (2006).
6. [https://www.sprawlsultrasound.org /production and interactions](https://www.sprawlsultrasound.org/production%20and%20interactions),10 -2015.
7. Thomas M. Deserno, “**Fundamentals of Biomedical Image Processing**”.
8. S.Kalaivani Narayanan and R.S.D.Wahidabanu,“**A View on Despeckling in Ultrasound Imaging**”,International Journal of Signal Processing, Image Processing and Pattern Recognition,Vol. 2, No.3, September 2009.

9. Raman Maini and Himanshu Aggarwal, **“A Novel Technique for Speckle Noise Reduction on Medical Images”**, International Journal of Applied Engineering Research ISSN 0973-4562 Volume 5 Number 1 (2010) pp. 1–8 © Research India Publications.

10. Khaled Z. Abd-Elmoniem, Student Member, IEEE, Abou-Bakr M. Youssef, and Yasser M. Kadah*, Member, IEEE, **“Real-Time Speckle Reduction and Coherence Enhancement in Ultrasound Imaging via Nonlinear Anisotropic Diffusion”**, IEEE TRANSACTIONS ON BIOMEDICAL ENGINEERING, VOL. 49, NO. 9, SEPTEMBER 2002.

11. Milindkumar V. Sarode and Prashant R. Deshmukh, **“Reduction of Speckle Noise and Image Enhancement of Images Using Filtering Technique”**, International Journal of Advancements in Technology Vol 2, No 1 (January 2011).

12. **Nishtha Atlas and Dr. Sheifali Gupta**, **“Reduction of Speckle Noise in Ultrasound Images using Various Filtering techniques and Discrete Wavelet Transform: Comparative Analysis”**, International Journal of Research (IJR) Vol-1, Issue-6, July 2014 ISSN 2348-6848.

13. Vaishali Kumbhakarna MPHIL (Computer Science) III Sem, Vijaya R. Patil MPHIL (Computer Science) III Sem, Dr. Seema Kawathekar (Asst. prof), **“Review on Speckle Noise Reduction Techniques for Medical Ultrasound Imaging Processing”**, international journal of computer techniques volume 12 issue 1, 2015.

14. Christos P. Loizou, Constantinos S. Pattichis, Robert S. H. Istepanian, **“comparative evaluation of despeckle filtering in ultrasound imaging of the carotid artery”**, October 2005.

15. R. VANITHAMANI, G. UMAMAHESWARI, and M. EZHILARASI, **“Modified Hybrid Median Filter for Effective Speckle Reduction in Ultrasound Images”**.

16. KINITA B VANDARA, and DR. G. R. KULKARNI, ENHANCEMENT“**METHODS FOR REDUCTION OF SPECKLE IN ULTRASOUND B- MODE IMAGES**”, JOURNAL OF INFORMATION, KNOWLEDGE AND RESEARCH IN ELECTRONICS AND COMMUNICATION ENGINEERING ISSN: 0975 – 6779| NOV 12 TO OCT 13 | VOLUME – 02, ISSUE - 02 Page 823.
17. V N Prudhvi Raj and Dr T Venkateswarlu, “**DENOISING OF MEDICAL IMAGES USING TOTAL VARIATIONAL METHOD**”, Signal & Image Processing: An International Journal (SIPIJ) Vol.3, No.2, April 2012.
- 18.1 Samir H. Abdul-Jauwad and 2 Mansour I. AlJaroudi,“**Wavelet Transform for JPG, BMP & TIFF**”.1 Electrical Engineering Department, King Fahd University of Petroleum & Minerals, 2 Electrical Engineering Department, King Fahd University of Petroleum & Minerals.
19. S. Sudha, G.R. Suresh and R. Sukanesh, “**Speckle Noise Reduction in Ultrasound Images by Wavelet Thresholding based on Weighted Variance**”, International Journal of Computer Theory and Engineering, Vol. 1, No. 1, April 2009.
20. [https://www.math.stackexchange.com/Fourier analysis](https://www.math.stackexchange.com/Fourier%20analysis),1-2016.
21. [https://zone.ni.com/WA Discrete wavelet transform](https://zone.ni.com/WA%20Discrete%20wavelet%20transform),3-2016.
22. [https://www.posterus.sk/edge detection using wavelet transform](https://www.posterus.sk/edge%20detection%20using%20wavelet%20transform),3-2016.
23. Zhao Hong-tu, Yan Jing, “**The Wavelet Decomposition And Reconstruction Based on The Matlab**”, Proceedings of the Third International Symposium on Electronic Commerce and Security Workshops (ISECS '10) Guangzhou, P. R. China, 29-31, July 2010.